

FINAL REPORT

for

DEVELOPMENT OF PILE TYPE, HIGH DISCHARGE RATE
NICKEL-CADMIUM SQUIB BATTERIES

MARCH 4, 1966 - AUGUST 4, 1967

CONTRACT NO.: NAS 5-10160

Prepared By

GULTON INDUSTRIES, INC.
ALKALINE BATTERY DIVISION
212 Durham Avenue
Metuchen, N. J.

For

GODDARD SPACE FLIGHT CENTER

Greenbelt, Maryland

FACILITY FORM 602

N67-39236
(ACCESSION NUMBER)
73
(PAGES)
CR-89327
(NASA CR OR TMX OR AD NUMBER)

(THRU)
1
(CODE)
03
(CATEGORY)

FINAL REPORT

for

DEVELOPMENT OF PILE TYPE, HIGH DISCHARGE RATE
NICKEL-CADMIUM SQUIB BATTERIES 4

MARCH 4, 1966 - AUGUST 4, 1967

CONTRACT NO.: NAS 5-10160

Prepared By

GULTON INDUSTRIES, INC.
ALKALINE BATTERY DIVISION
212 Durham Ave.
Metuchen, N. J.

for

GODDARD SPACE FLIGHT CENTER
Greenbelt, Maryland

Prepared By:



S. Charlip
Section Head
Engineering Development



A. Lyall
Senior Chemical Engineer

Approved By:



H. N. Seiger
Director of Research



R. C. Shair
Vice President
Research & Development

ACKNOWLEDGEMENT

The authors wish to acknowledge the contributions of Messrs. T. Staub and A. Jakubczak of the Gulton R & D Staff in this investigation.

DEVELOPMENT OF PILE TYPE, HIGH DISCHARGE RATE,
NICKEL-CADMIUM SQUIB BATTERIES

by

S. Charlip and A. Lyall

ABSTRACT

The objective of this program is the development of small size, thick sinter, five cell bipolar nickel-cadmium, sealed, rechargeable batteries to deliver a one second pulse at 10 amperes above 5 volts for squib activation. A minimum capacity of 150 mAh at the 10-hour rate was required.

The report emphasizes the work of developing thick bipolar electrodes, .030 inch sinter, in circular shapes, capable of being impregnated to a capacity of 150 mAh/in² of sinter area.

The development of a bonded rubber-to-metal seal permitted the construction of ten 5-cell modules, fully encapsulated, which yielded several pulses with current densities of 3.6 A/in² above 5 volts, for electrode sizes of 2.76 in².

Single bipolar cells and five-cell batteries were tested, vented, and sealed. Based on laboratory cell test data, concentration and activation polarization are the limiting parameters of current density outputs in a bipolar nickel-cadmium battery.

Further investigation which would lead to an optimized system with overcharge capabilities is recommended.

TABLE OF CONTENTS

	<u>PAGE NO.</u>
ABSTRACT	iii
INTRODUCTION	1
DEVELOPMENT OF BIPOLAR ELECTRODES	3
Development of the Bipolar Sintering Process	3
<u>Slurry Sintering</u>	3
<u>Loose Sintering</u>	5
<u>Controlling Sinter Porosity</u>	5
Development of Impregnation Techniques	7
<u>Positive Electrode Impregnation</u>	7
<u>Negative Electrode Impregnation</u>	7
Formation	8
SINGLE CELL EVALUATION-SUMMARY OF TEST DATA	9
<u>Capacity Discharges</u>	9
<u>Pulse Discharges of 4 in² Cells</u>	9
<u>Pulse Discharges of Smaller Cells</u>	14
EVALUATION OF FIVE-CELL BATTERIES	26
Adhesive Bonding	34
<u>Surface Treatment</u>	34
<u>Adhesives and Seal</u>	36
<u>Assembly Procedures & Test Results of</u>	
<u>10 Development Batteries</u>	38
DISCUSSION OF RESULTS AND CONCLUSIONS	51
RECOMMENDATIONS	52
REFERENCES	53
APPENDIX I - CALCULATIONS OF HEAT RISE DUE TO DISCHARGE CURRENT	

LIST OF FIGURES

<u>FIGURE NO.</u>		<u>PAGE NO.</u>
1	Construction of a Bipolar Battery	2
2	Atmosphere Controlled Continuous Feed, Sintering Furnace for Bipolar Electrodes	4
3	Typical Mold Design for Bipolar Plates	6
4	Test Set-up For Single Cell With Bipolar Plates	10
5	Discharge of Bipolar Cell - 2-1/4 In. Dia. Active Area at the C Rate, 600 mA, at Room Temp.	11
6	Pulse Discharge of Single Bipolar Cell With 4 Square Inches of Active Plate Area	12
	a. Pulse 1	
	b. Pulse 2	
7	Pulse Discharge of Single Bipolar Cell With 4 Square Inches of Active Plate Area	13
	a. Pulse 6	
	b. Pulse 1	
8	High Current, Low Voltage Discharge Apparatus	15
9	Motor Driven Switch	16
10	Pulse Discharge For a Single Bipolar Cell With 2.07 Square Inches of Active Plate Area	18
	a. Pulse 1	
	b. Pulse 2	
11	Oscilloscope Traces of 4 Square Inch Bipolar Bipolar Electrodes	19
	a. Load 0.0447 Ohms	
	b. Load 0.0244 Ohms	
	c. Load 0.0155 Ohms	
12	Voltage-Current Relationship, Single Bipolar Cell With 4 Square Inches of Active Area	20
13	Electrode to Reference Pulses, All Load at 0.0244 Ohms	21
14	Pulse Discharge of a Single Bipolar Cell With 2.40 Square Inches Active Plate Area	23
	a. Pulse 1	
	b. Pulse 2	

List of Figures - Continued

<u>FIGURE NO.</u>		<u>PAGE NO.</u>
15	Pulse Discharge of a Single Bipolar Cell With 2.76 Square Inches of Active Plate Area a. Pulse 1 b. Pulse 2	24
16	Pulse Discharge For a Single Bipolar Cell With 3.14 Square Inches Active Plate Area, Current 10.5 Amperes	25
17	Five Cell Battery With 2 Square Inches of Sinter Area	27
18	Charge and Discharge of a 5-Cell Battery Showing Average Cell Voltage and Spread	28
19	Pulse Discharge for a 5-Cell Bipolar Battery With Active Plate Area of 2.07 Square Inches a. Pulse 1 b. Pulse 2	29
20	Cross-Sectional View of a Bipolar Cell Assembled With a "Quad" Ring Seal	31
21	Pulse Discharges for a 5-Cell Bipolar Battery With 2.40 Square Inches Positive and 2.07 Square Inches Negative Active Plate Areas	32
22	Oscilloscope Traces for a Pulse Discharge of a 5-Cell, 4 Square Inch Bipolar Battery	33
23	Flow Chart for Surface Preparation of Nickel Substrates for Bipolar Batteries	35
24	Cross-Sectional View of a Rubber-To-Metal Seal In a Bipolar Cell	37
25	Wabash Press With Heated Plattens for Vulcan- izing Rubber Seals	39
26	Half-Mold for Vulcanizing Rubber Seal to Substrate of Bipolar Electrode	40
27	Oscilloscope Traces for 8 Consecutive Pulse Discharges of a 5-Cell, Vented, 3.1 Square Inch Bipolar Battery a. Pulse 1 b. Pulse 3, 5, 7, and 8	42
28	Oscilloscope Traces for 2 Consecutive Pulse Discharges of a 5-Cell, Vented, 2.76 Square Inch Bipolar Battery a. Pulse 1 b. Pulse 2	43

List of Figures - Continued

<u>FIGURE NO.</u>		<u>PAGE NO.</u>
29	Oscilloscope Traces for 13 Consecutive Pulse Discharges of a 5-Cell, Sealed, 3.1 Square Inch Bipolar Battery	44-46
	a. Pulse 1	
	b. Pulse 2	
	c. Pulse 3	
	d. Pulse 4 thru 10	
	e. Pulse 11	
	f. Pulse 13	
30	Oscilloscope Traces for 2 Consecutive Pulse Discharges of a 5-Cell, Sealed, 2.76 Square Inch Bipolar Battery	47
	a. Pulse 1	
	b. Pulse 2	
31	Five-Cell, 10 Ampere Pulse Discharge Bipolar Battery	48
32	Oscilloscope Traces for 2 Consecutive Pulse Discharges of a 5-Cell, 2.76 Square Inch Sealed and Encapsulated Bipolar Battery	50
	a. Pulse 1	
	b. Pulse 2	

INTRODUCTION

The bipolar battery derives its name from its electrode configuration which contains the positive element of one cell and the negative element of the next cell on two sides of a conducting thin sheet called the substrate. The substrate, in addition to being the current collector of each electrode, also acts as the intercell connector between two adjacent cells. A series of such bipolar electrodes, positioned so that a positive electrode surface and a negative electrode surface of adjacent plates are facing each other through an ionic separator and electrolyte, make up a pile battery. The voltage of the battery is a function of the number of bipolar plates stacked in a pile. Figure 1 shows a typical configuration of a bipolar electrode pile type battery.

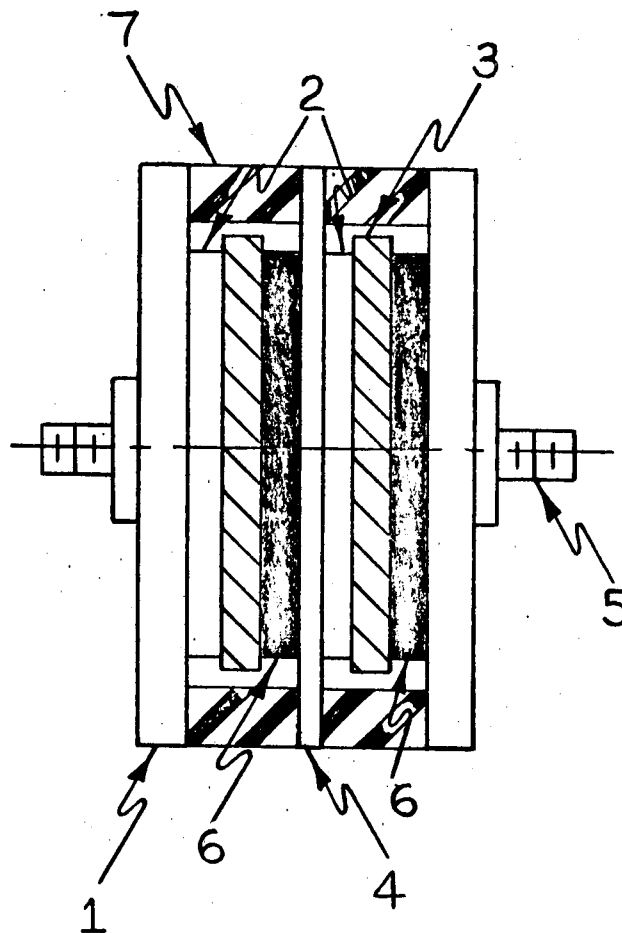
Because of their unique geometric features and the absence of inter-cell connectors, pile type batteries possess relatively low internal impedance values and are capable of higher rates of discharge at given voltage levels.

Bipolar cells have evolved, historically, from the original Volta battery which had a bipolar configuration. It consisted of a series of cells made by placing common salt moistened cloth separators between copper and zinc discs, stacked in a pile⁽¹⁾. High current densities, from a bipolar pile type battery in the lead-acid system, were obtained and described in 1924 by the Russian physicist Kapitza⁽²⁾.

A study of high current densities in bipolar batteries with large area, thin foil type electrodes, was made by Gulton Industries in 1966 for the U. S. Army Missile Command. The results were published in a Final Report⁽³⁾. The purpose of the study was to expand on the experimental work published in 1956 by Willingham⁽⁴⁾. The objectives of the work covered by this contract were to develop sealing laws and fabrication techniques for small size bipolar batteries with thick electrode sinters which would ultimately lead to the fabrication of five-cell pile type batteries capable of at least one 50 watt pulse of one second duration, at a minimum voltage of five volts, and a capacity of 150 mAh at a ten hour rate.

The work described in this report deals with the development of thick sintered (30 mil) bipolar electrodes and the extension of these techniques to bipolar battery technology of sealed five-cell modules.

In order to achieve the stated objectives, it was first necessary to make progress in the areas of bipolar battery electrodes, sealing materials and processes, and assembly techniques. Each area is described in the body of this report.



1. SUBSTRATE *for* END PLATE
2. SINTERED MATRIX-Ni OXIDE POS. PLATES
3. SEPARATOR
4. SUBSTRATE *for* INTERIOR PLATE
5. END TERMINAL
6. SINTERED MATRIX-CADMIUM NEG. PLATES
7. SEAL

FIG. 1 CONSTRUCTION *of* A BIPOLAR BATTERY

DEVELOPMENT OF BIPOLAR ELECTRODES

Development of the Bipolar Sintering Process

The manufacture of bipolar electrodes requires new and different techniques from those of standard batteries. The construction of the sintered type nickel-cadmium battery electrode consists of depositing a nickel sintered matrix over both sides of a perforated substrate sheet by immersing it in a slurry of nickel powder. The wet slurry sheet is then dried, sintered, and subsequently cut to the desired electrode size. The resultant electrode, which is now ready for impregnation with active materials, is a porous carrier with a nominal thickness between .020 to .030 inch.

In order to deposit a spongy nickel sinter on each side of the solid sheet substrate, the sinter has to be deposited on each side separately. It was required, therefore, to develop sintering techniques for the processing of a single side at a time. All electrodes were constructed with .021 inch thick nickel substrates and .030 inch sinter thickness on each side. All electrodes were round discs and ranged in size from 2-1/4 inches in sinter diameter (approximately 4 in² of active area) to 1-5/8 inches in sinter diameter (approximately 2 in² of active area). These sizes were considered as the maximum and minimum practical ranges for the application. Intermediate sizes, varying in diameter by 1/8 inch, were also constructed. Each bipolar plate, or end plate, had a border of 1/4 inch free from sinter for sealing. Thus, the 2-1/4 inch sinter had a substrate of 2-3/4 inches in diameter.

The sintering of all plates was done in a continuous feed furnace, atmospherically controlled. The furnace and controls were specifically designed for sintering bipolar electrodes. A photograph of this furnace is shown in Figure 2. The electrodes were fired in a dry atmosphere containing a mixture of 80% nitrogen and 20% hydrogen. The methods used for applying the nickel powder to the plates were as follows:

Slurry Sintering

The first electrodes, 4 in², were sintered using this technique. It consisted of placing a slurry of nickel powder in an organic binder onto a substrate by filling the cavity of a plastic mold placed on one side. The electrode was allowed to dry in the mold, the mold removed, and the plate with the powder fired in the furnace. The process was repeated for the second side. It was found, in an earlier program⁽³⁾, that this process was not readily adaptable to thin sheets and sinters, due to shrinkage of the powder which caused poor adhesion. However, using a thicker substrate, .021 inch, the problem of adhesion was minimized. Due to the high shrinkage rate, uniform porosity of sinters could not be controlled in the thicker plates.



FIGURE 2. ATMOSPHERE CONTROLLED CONTINUOUS FEED,
SINTERING FURNACE FOR BIPOLAR ELECTRODES

OPERATOR - LOADING A PLATE

Loose Sintering

This technique consisted of filling a mold with nickel powder, then leveling the mold so that the desired thickness was obtained. No wetting agents were used. The bond and the desired porosity levels were achieved by varying the temperature and time cycles. A typical mold design is shown in Figure 3. Initial sample lots indicated that this method of sintering could be used to obtain good adhesion and controlled porosity.

Controlling Sinter Porosity

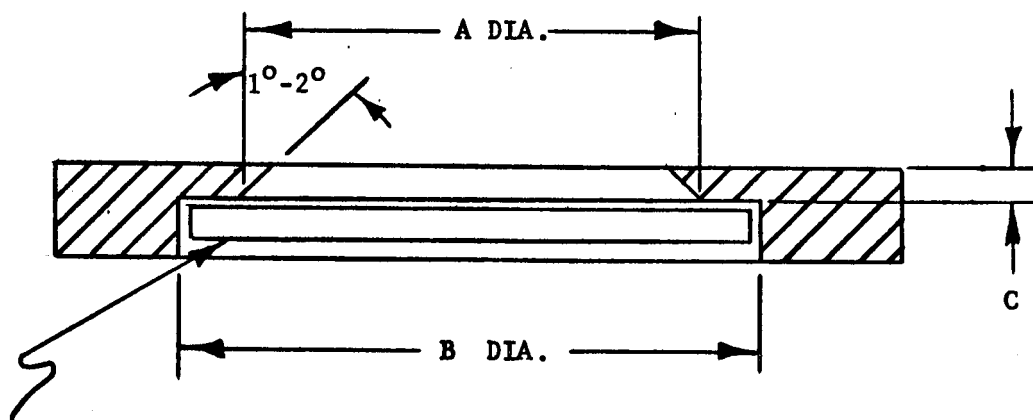
The porosity levels and uniformity of sinters were controlled by varying the time-temperature cycles on sintering, and thus, the shrinkage of the nickel powder. Because each side of a bipolar plate was fired separately, the second side was exposed to the temperature-time cycle twice, and showed greater shrinkage. To obtain uniform shrinkage on each side, the heating cycles were modified on the second side. Literature⁽⁵⁾ indicated that temperature has a greater effect on volume shrinkage (porosity) of nickel powders than does time. Keeping the sintering time constant, the electrodes were fired at a higher temperature on the first side than on the second side. This procedure gave sinter porosities in the range of 80% to 82% in samples tested. It is important, for good performance, that porosity of sinters be uniformly controlled. Higher porosity levels than those established are normally associated with large openings in the sponge-like sinter material, which may impair the ability of the sinter to hold the active materials due to lack of capillary attractive force. Lower porosity levels, or high density sinters, will offer little volume for the active materials. The uniformity of the porosity levels is necessary for the cells to have equal capacities, since they will hold equal volumes of active materials.

The levels of porosity in the sinters were determined from the amount of toluene that the sinter could hold. Toluene was used because of its moderate boiling point (110.6°C), low surface tension (28.5 dynes/cm at 20°C; water has a surface tension of 72.05 dynes/cm), and low viscosity (0.590 Cp at 20°C). These properties permit rapid penetration into small pores and a slow rate of evaporation.

After measuring the volume of the sinter and weighing each bipolar plate in the dry condition, it was wetted with toluene and the excess blotted with bibulous paper. The bipolar plate was then rapidly reweighed. From the recorded weight of absorbed toluene (knowing the specific gravity), the total volume of absorbed liquid was computed. The plate porosity was calculated from the ratio of absorbed volume of toluene to the total volume of the plate:

$$\% \text{ Porosity} = \frac{\text{Volume of toluene}}{\text{Volume of total sinter}} \times 100$$

Several batches of consecutively sintered plates were examined and tested for adhesion and uniformity of sinter. The plates were found to have good adhesion and uniform consistency.



NICKEL SUBSTRATE SHEET

A DIA. = Dia. Of Desired Sintered Area Plus 17%

B DIA. = Dia. Of Substrate Sheet Plus .015 inch

C = Thickness of Sintered Area Plus 26%

FIGURE 3 TYPICAL MOLD DESIGN FOR BIPOLAR PLATES

Development of Impregnation Techniques

The impregnation of bipolar electrodes differs considerably from that of standard plates in the nickel-cadmium battery system. Standard nickel-cadmium electrodes are impregnated by the process of immersion in a tank filled with an appropriate solution containing the precursors of the active materials. Each electrode (positive or negative) is immersed separately in a different solution, and the amount of active material absorbed by the electrode is measured by the weight gain.

This technique could not be used for impregnating bipolar plates since both electrodes (positive and negative) are on opposite sides of the same sheet. It became necessary to develop new techniques for the impregnation of the bipolar plates. These consisted of hand applications of a chemical solution for both negative and positive electrodes. The method of application is described below.

Positive Electrode Impregnation

The impregnation of the positive electrode (positive side of the bipolar plate) was accomplished by successive applications of nickel salt solutions with good wetting properties which were readily absorbed by the sinter.

A total of eight applications were required to impregnate the positive electrode to the desired level. After each impregnation, the electrode was thoroughly dried, then converted to nickel hydroxide with a hot (140°F) sodium hydroxide solution. The electrode was rinsed to neutral (pH 7.0) with deionized water and dried before the next impregnation. Since usable capacity is only 80% of theoretical, the impregnation was calculated to compensate for the loss in efficiency.

The electrodes were impregnated to their practical limit, which is approximately 75% of the free theoretical volume. The following are the average weight gains for 4 in² electrodes (2-1/4 inch diameter sinter), found by weighing each electrode before and after impregnation.

ELECTRODE	GAIN IN ACTIVE MATERIALS	EQUIV. THEORETICAL CAPACITY IN mAh
Positive	2.60 grams	750

Negative Electrode Impregnation

The impregnation of the negative side of the bipolar plate was accomplished in a manner similar to the positive side. A concentrated solution of cadmium nitrate [Cd(NO₃)₂] was used for the impregnation of the negative electrodes. Four successive applications were required to impregnate the negative electrode. Each application was followed by a conversion in sodium hydroxide and prolonged washing and drying cycles.

The average weight gains of the negative electrodes with 4 in² of sinter were found to be as follows:

ELECTRODE	GAIN IN ACTIVE MATERIALS	EQUIV. THEORETICAL CAPACITY IN mAh
Negative	1.64 grams	600 - 680

The positive material is about 80% utilizable, which yields 600 mAh. The range of the negative capacity is due to the degree of dehydration of the Cd(OH)₂ to CdO which occurs on drying. The utilization here is better than 90%.

The theoretical capacities of smaller electrodes, with 30 mil thick sinters and active areas less than 4 in², were proportional to those shown above. Thus, an electrode with 2 inches in diameter (3.1 in² of active area) was impregnated to a theoretical capacity of 450 mAh, and one with 1-3/4 inch diameter (2.4 in²) to 350 mAh. The capacity of a bipolar multicell battery is, of course, limited by the capacity of the lowest cell or electrode.

Formation

Nickel-cadmium electrodes must initially be subjected to electrochemical activity alien to cell use. This is necessary to convert the "chemically" formed passive nickel hydroxide [Ni(OH)₂] and cadmium hydroxide [Cd(OH)₂] to the more active "electrochemically" formed hydroxides. This improves the coulombic efficiency (available energy from theoretical energy) of the nickel-cadmium cell.

The formation of the squib battery electrodes was accomplished through repeated charging and discharging of opposite sides of the bipolar plates while they were immersed in an open tank containing potassium hydroxide.

The charging was performed with a constant current power supply at the C rate to an end voltage coincident with a downward break in the voltage curve. Each side of the bipolar plate was given a total of three full charge-discharge cycles. Following the third cycle, the plates were brought to electrochemically zero potential so that, during assembly into a test cell, the plates would be in an electrochemically neutral state.

SINGLE CELL EVALUATION - SUMMARY OF TEST DATA

In order to evaluate ultimate battery performance, single test cells were constructed. These cells were made up from two end plates, one impregnated with positive and the other with negative materials. Each end plate, therefore, was in essence a half of a bipolar electrode with the other side left smooth for electrical connections and packaging. Cells were assembled with separators of non-woven nylon and sandwiched between two bolted plastic plates which exerted pressure on the cell and maintained intimate contact between the electrode and the wet separator. The entire package was placed in a container filled with KOH solution.

The extending terminals of the test cells were connected to a constant current power supply and charged at 600 mA for one hour, to a terminal voltage of 1.59 volts. Figure 4 shows a typical test set-up for single cells.

Capacity Discharges

First cells built were constructed of end plates with 4 in^2 active area. Their capacities were determined by discharging at a constant current of 600 mA to terminal voltages of 1.0 volts. Figure 5 shows a discharge curve of a 4 in^2 bipolar cell made from two end plates. The capacity here is 600 mAh.

Smaller plates with 2 in^2 of sinter area (1-5/8 inch diameter) were impregnated to an average weight gain of 0.7 grams of positive material, equivalent to a theoretical capacity of 202 mAh. The negative electrode gained an average of 0.9 grams, equivalent to a theoretical capacity of 326 mAh. Actual discharge capacity of single flooded cells made from end plates yielded from 150 to 165 mAh.

The capacity, therefore, for any size under consideration was sufficient to satisfy the 150 mAh requirement.

Pulse Discharges of 4 in^2 Cells

To ascertain cell performance to yield high rate pulse discharges, fully charged test cells, made up of bipolar end plates, were connected to loads which produced a 10 ampere drain. The cell terminals were also connected to a Brush Recorder to read voltage and time intervals of one second duration. Because of calibration adjustments, actual drains were somewhat higher than the 10 amperes expected. Likewise, time intervals were longer than one second.

Figures 6a and 6b are the graphs of two consecutive pulse discharges of a flooded 4 in^2 bipolar cell. The cell was pulsed for a total of 28 consecutive pulses (without recharging). The first six pulses were above one volt. The following 22 pulses were slightly below the minimum of one volt per cell (5 volts per battery). Pulse No. 6 is shown in Figure 7a. A 20 ampere pulse discharge of the same cell (after recharging) is shown in Figure 7b.

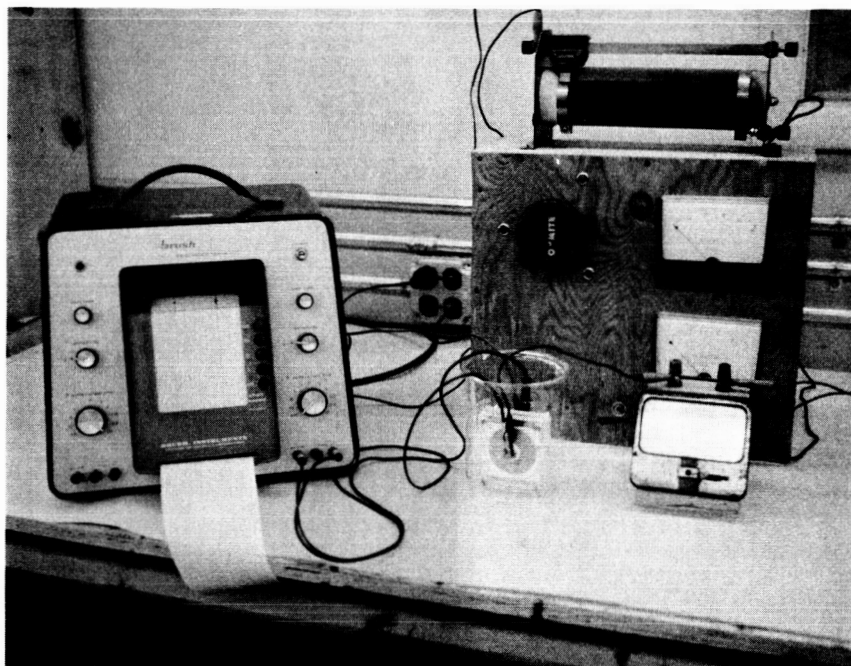


FIGURE 4.

TEST SET-UP FOR SINGLE CELL WITH BIPOLAR PLATES

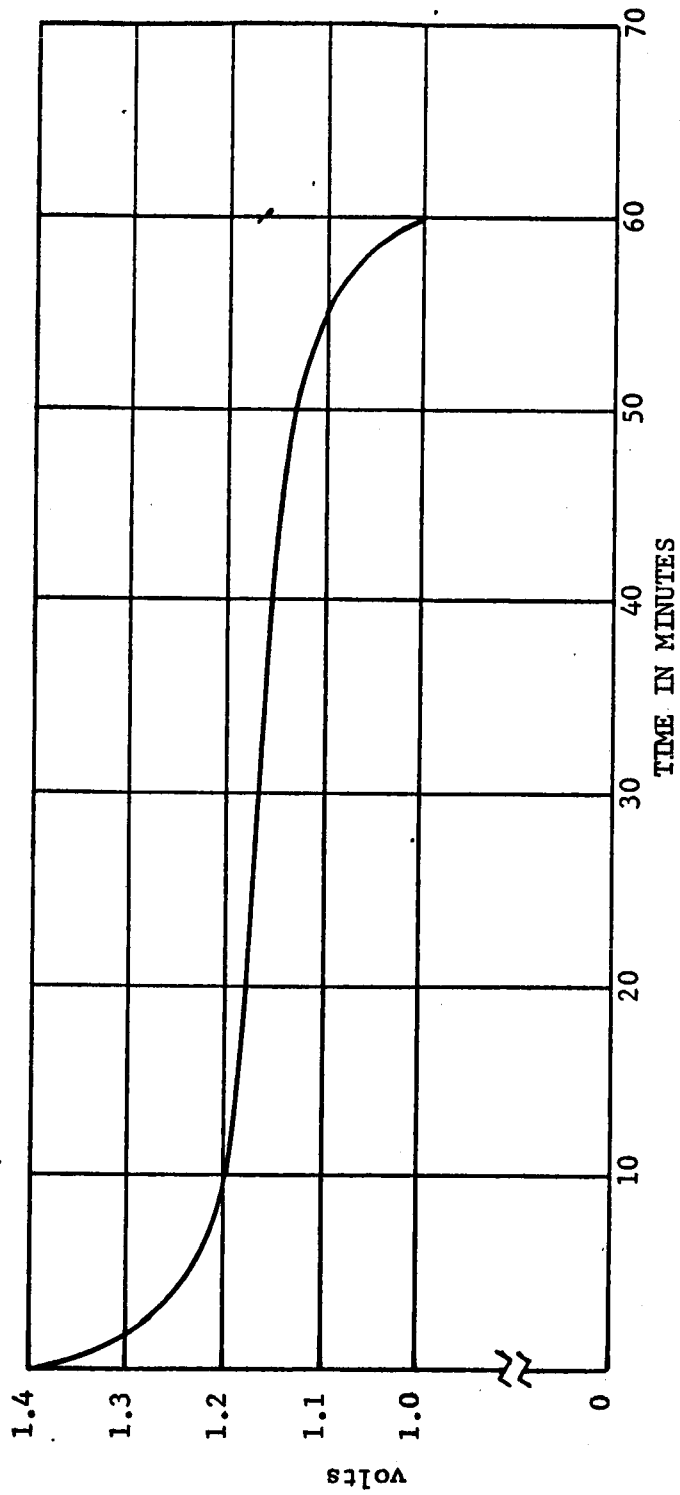


FIGURE 5 DISCHARGE OF BIPOLAR CELL - $2\frac{1}{2}$ INCH DIAMETER ACTIVE AREA
AT THE C RATE, 600 mA, AT ROOM TEMPERATURE

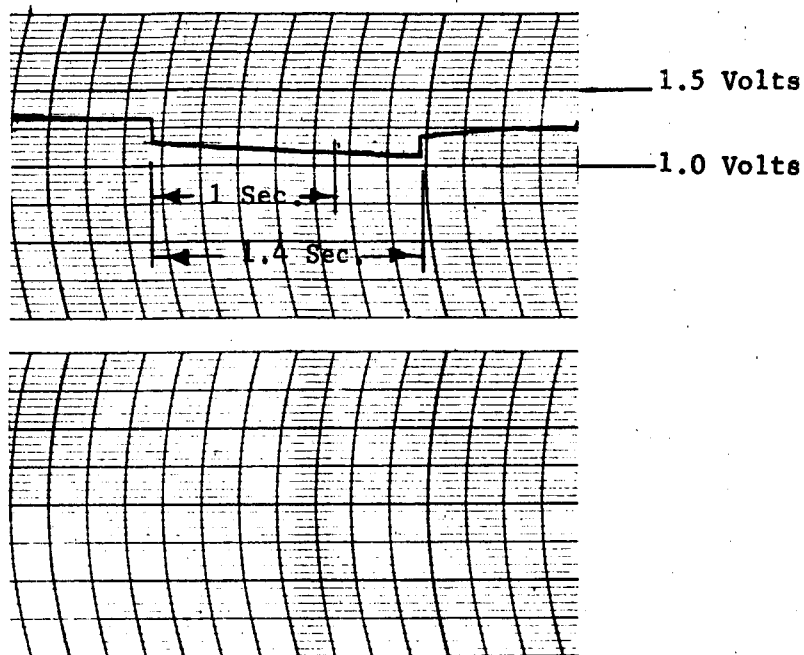


FIGURE 6a

PULSE 1 CURRENT - 11.5 AMPERES

PULSE DISCHARGE OF SINGLE BIPOLAR CELL
WITH 4 SQUARE INCHES OF ACTIVE PLATE AREA

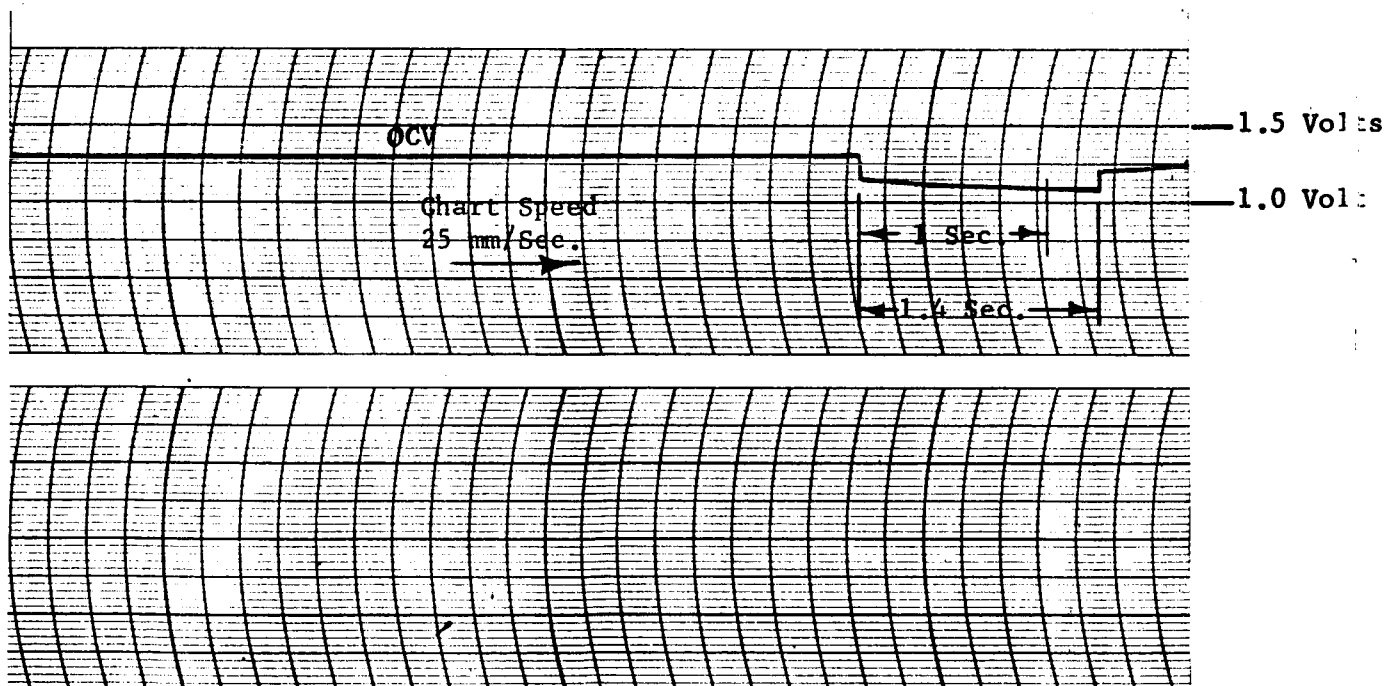


FIGURE 6b

PULSE 2 CURRENT - 11.5 AMPERES

PULSE DISCHARGE OF SINGLE BIPOLAR CELL WITH
4 SQUARE INCHES OF ACTIVE PLATE AREA

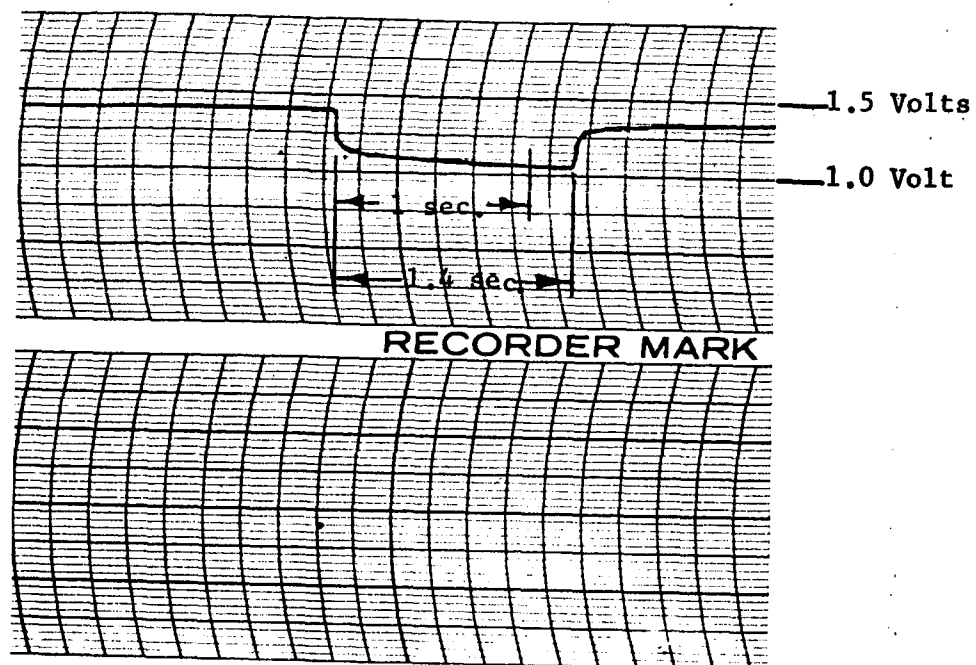


FIGURE 7a

PULSE 6

CURRENT - 11.5 AMPERES

PULSE DISCHARGE OF SINGLE BIPOLAR CELL WITH
4 SQUARE INCHES OF ACTIVE PLATE AREA

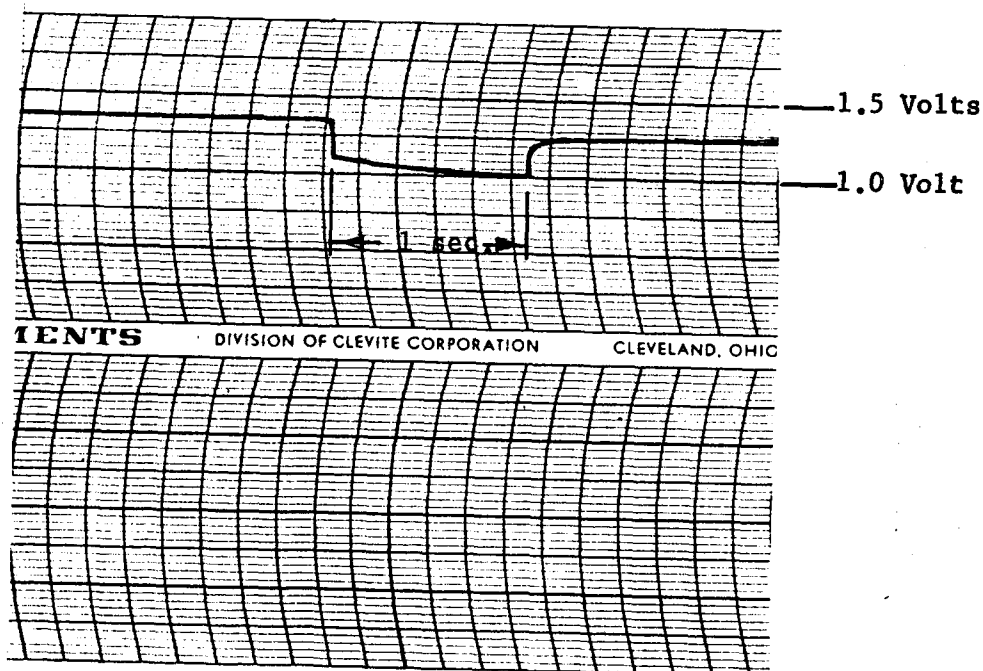


FIGURE 7b

PULSE 1

CURRENT - 20 AMPERES

PULSE DISCHARGE OF SINGLE BIPOLAR CELL WITH
4 SQUARE INCHES OF ACTIVE PLATE AREA

The current density of the cell with 4 in² of active area gives:

$$\text{Current density} = \frac{\text{Current}}{\text{Area}} = \frac{11.5 \text{ amperes}}{4 \text{ in}^2} = 2.87\text{A/in}^2$$

to 1.0 volt, for the pulses in Figure 6.

For the 20 ampere discharge, the current density is 5 A/in² to 1.0 volt. However, the voltage on subsequent pulses would drop below the one volt level.

Pulse Discharges of Smaller Cells (3.1 In² to 2 In²)

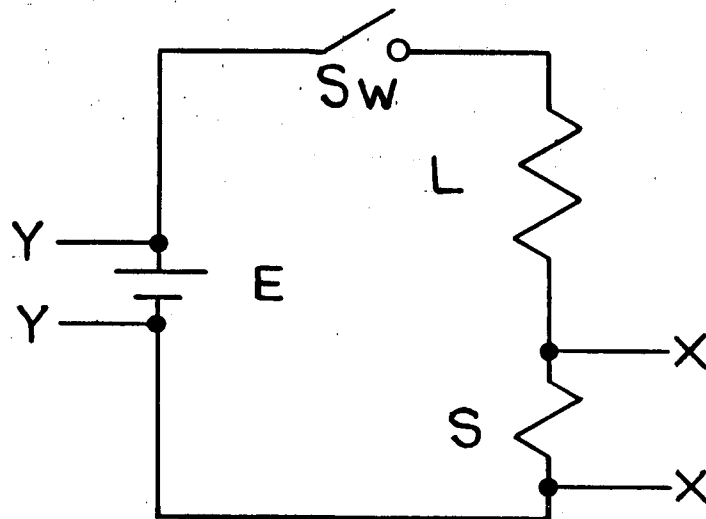
It would seem logical to suspect that if the area and the current were reduced by half, the current density would remain constant, and therefore, the voltage would also remain unchanged.

Flooded cells, constructed from bipolar end plates (sintered on one side only) with 2 in² of active area (circular plates of 1-5/8 inch diameter of sinter) were constructed and assembled with 7 mil separators of non-woven nylon. The cells were clamped between two plastic blocks and immersed in a beaker containing a 34% solution of KOH. Two nickel tabs, spotwelded to the end plates, protruded above the electrolyte and connected to test equipment.

Two types of test procedures were used to evaluate the current voltage relationships. The first consisted of actual pulse discharge of 10 amperes for one second, the same as for the 4 in² plates. In this procedure, the cell under test was backed up by a high capacity (35 Ah) battery of 28 volts to sustain a constant current regardless of the voltage changes in the test cell.

The second type of test consisted of pulse discharges of 20 milliseconds duration through a fixed load. This test has an advantage in that the test cell is supplying the energy and is not acting as a resistor, which it does during a forced discharge. In some instances, discrepancies were observed between the two methods. As a check of the first test method, a series of pulse discharges were conducted using the second method. For a better understanding of the problem, (current density as a function of electrode area) reference electrodes were used with the fixed load pulses.

Figure 8 shows a schematic diagram of a circuit for pulse discharges of short duration. The key element in the circuit is the switch (SW). In order to obtain a good contact for a short time, a rotary switch was made. A diagram of this switch is shown in Figure 9. The switch was driven by a 27 RPM motor with adjustable contacts, controlled by spring tension. The contact time was set by adjusting the angle of the contact arm and the spring tension. The load bank ("L") was set to correspond to the discharge conditions, and the shunt ("S") measured the current flowing in the circuit.



E = Bipolar Battery
 SW = Rotating Switch
 L = Load Back
 S = Shunt
 XX = To Oscilloscope for Current Measurement
 YY = To Oscilloscope for Voltage Measurement
 /

FIGURE 8 HIGH CURRENT - LOW VOLTAGE DISCHARGE APPARATUS

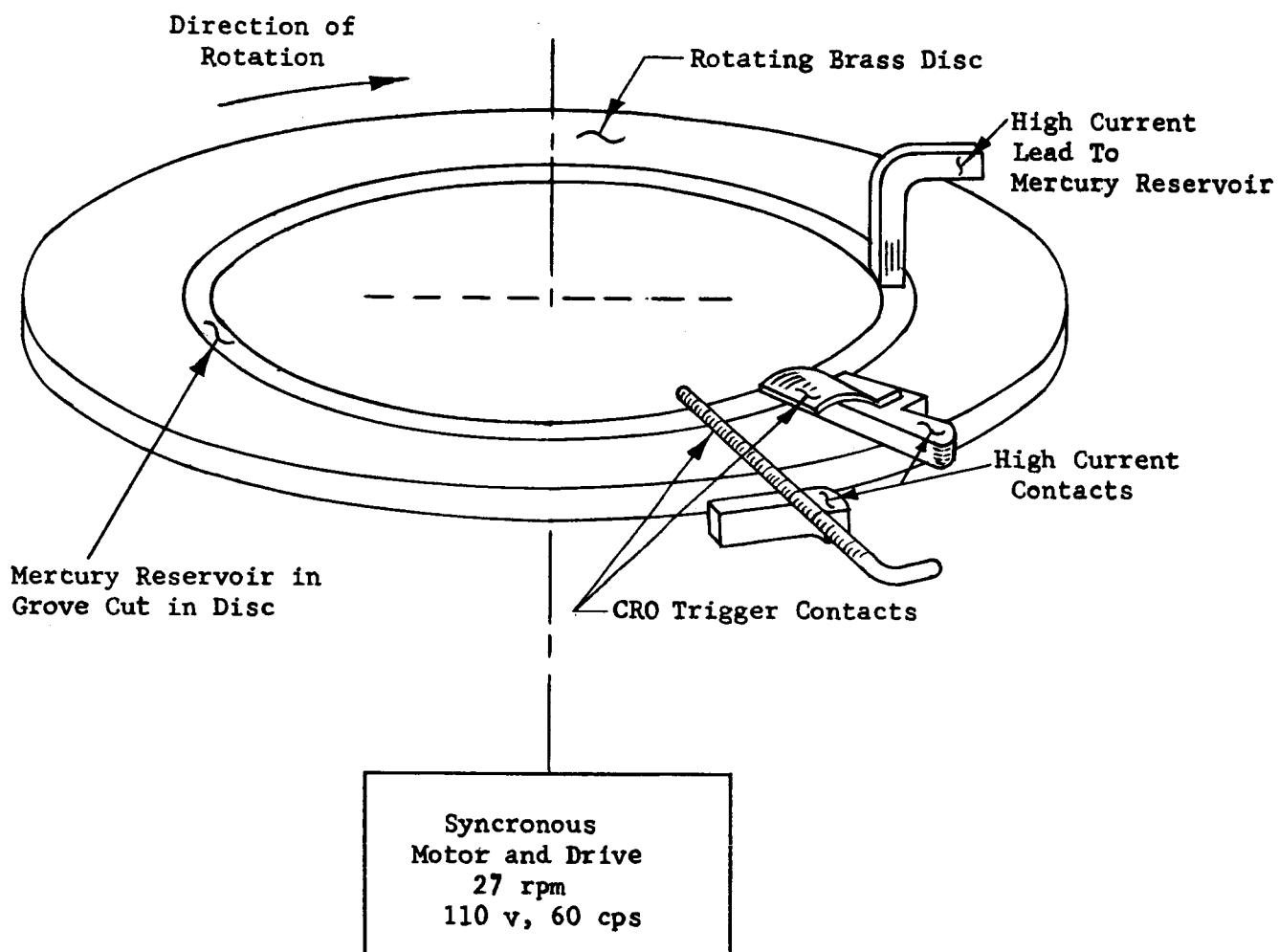


FIGURE 9.

MOTOR DRIVEN SWITCH

The terminal load was measured prior to discharge using a Mueller Bridge. The current was measured across the shunt and cell voltage calculated, or cell voltage measured across the terminals and battery voltage calculated. To avoid the effects of distributed load and terminal resistance of the cell, voltage and current were not measured simultaneously in this experiment. However, in later tests the circuit was improved to permit both measurements simultaneously.

Figures 10a and 10b are pulse discharge traces of a single flooded cell with 2 in² of active area. The cell was charged at 15 mA for 16 hours and then pulsed at 10 amperes (forced discharge) with the voltage recorded on a Brush Recorder Mark II. Subsequent tests gave similar results. The cell voltage was just below the 1.0 volt level at the end of one second. This is below the expected level based on the results obtained with a 4 in² cell pulsed at 20 amperes.

The test with the 4 in² plates was duplicated using the second test method. A fully charged cell was pulsed at fixed loads using an oscilloscope and a camera to record the current. Figure 11 shows oscilloscope traces of the discharges. Calculating the voltage drops at these currents, the resulting cell voltage of 1.28 volts is assumed at zero current, since this is the normal open circuit voltage of a nickel-cadmium cell after several days on stand. Calculating the voltage drops at these currents, the resulting cell voltage was plotted on a graph, shown in Figure 12. The results show that at 10 amperes, a cell voltage of 0.98 volts can be expected for the 2 in² cells, which is consistent with the forced discharge results.

To gain knowledge about the behavior of each individual electrode, a series of pulse discharges were conducted using a Hg/HgO reference electrode.⁽⁶⁾ The traces in Figure 13 show the negative electrode as highly polarized ($\Delta V = 0.66$ volts) at the start of the discharge, then recovers about 0.1 volt during the first 8 milliseconds. The positive electrode shows a drop of 0.25 volt after one millisecond, and continues to decrease, with time, at a rate greater than the recovery of the negative. The combination results in a steady decrease of cell voltage with time. Figure 13b shows that there is very little change in current during the pulse duration. However, the current varies with the voltage at the constant load, unlike a forced discharge at constant current.

The tests with the reference electrode show the presence of activation polarization in both electrodes--slightly higher in the negative than in the positive electrode. However, the positive electrode, which is greatly susceptible to concentration polarization, shows the presence of this polarization by the voltage drop increase with time.

To rule out the possibility of a "state of charge" effect, a cell was subjected to three consecutive pulses at one minute intervals without recharging. The discharge traces are shown in Figure 13d. These traces are almost superimposed on each other, and show no change in the rate of decay with the state of charge.

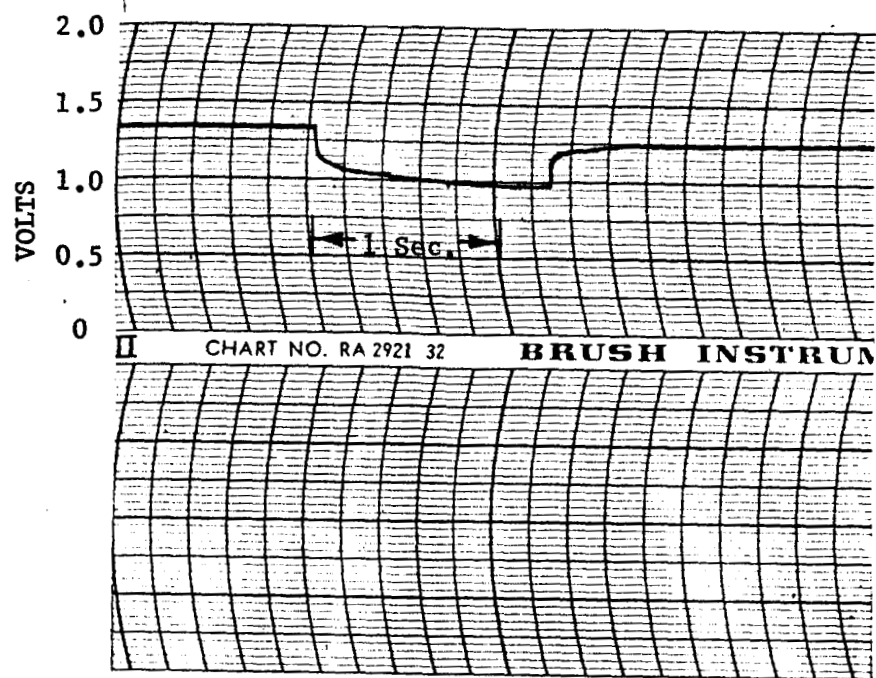


FIGURE 10a PULSE NO. 1 10 AMPERES
PULSE DISCHARGE FOR A SINGLE BIPOLAR CELL
WITH 2.07 IN² ACTIVE PLATE AREA

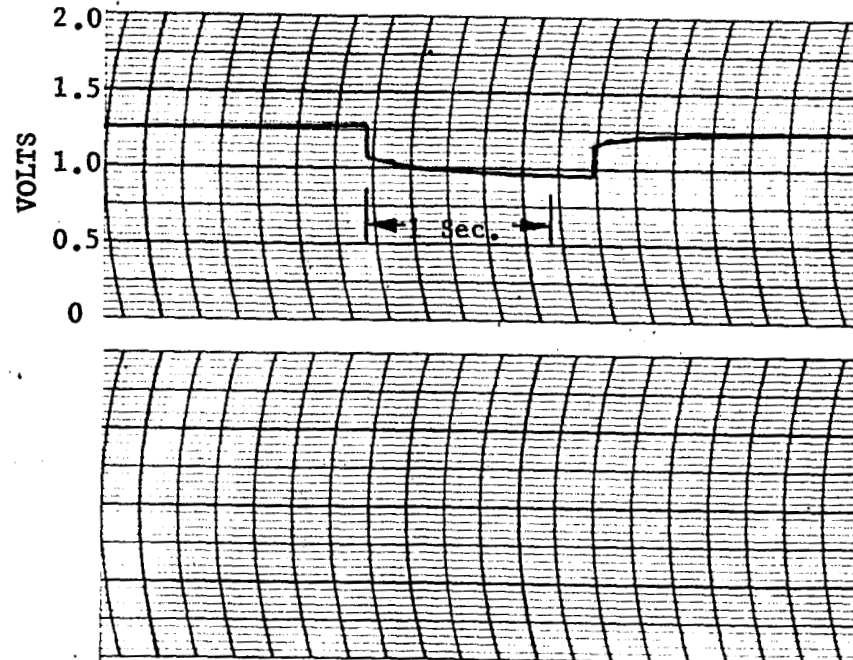


FIGURE 10b PULSE NO. 2 10 AMPERES
PULSE DISCHARGE FOR A SINGLE BIPOLAR CELL
WITH 2.07 IN² ACTIVE PLATE AREA

AMPERES
60
40
20
0

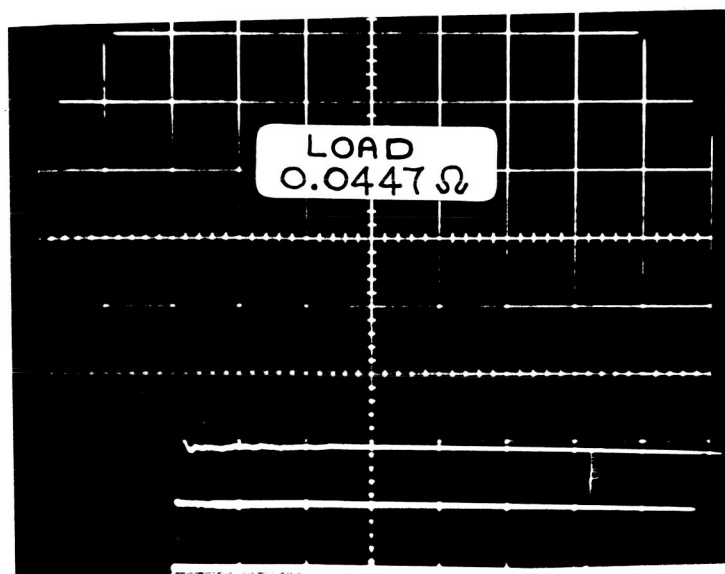


FIGURE 11a

AMPERES
60
40
20
0

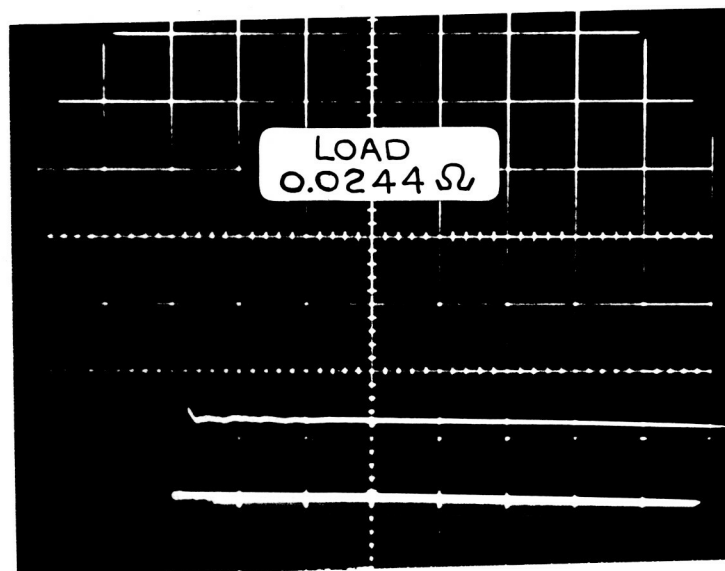


FIGURE 11b

AMPERES
60
40
20
0

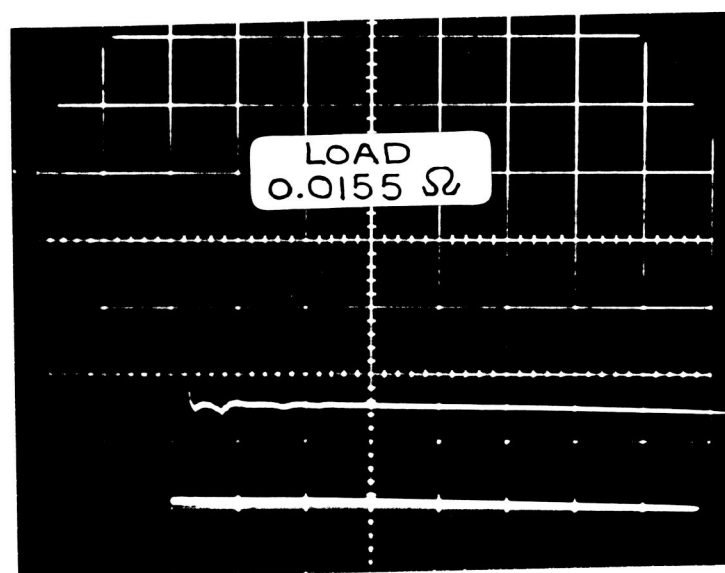


FIGURE 11c

0 1 2 3 4 5 6 7
TIME IN MILLISECONDS

(OSCILLOSCOPE TRACES OF 4 SQUARE INCH
BIPOLAR ELECTRODES)

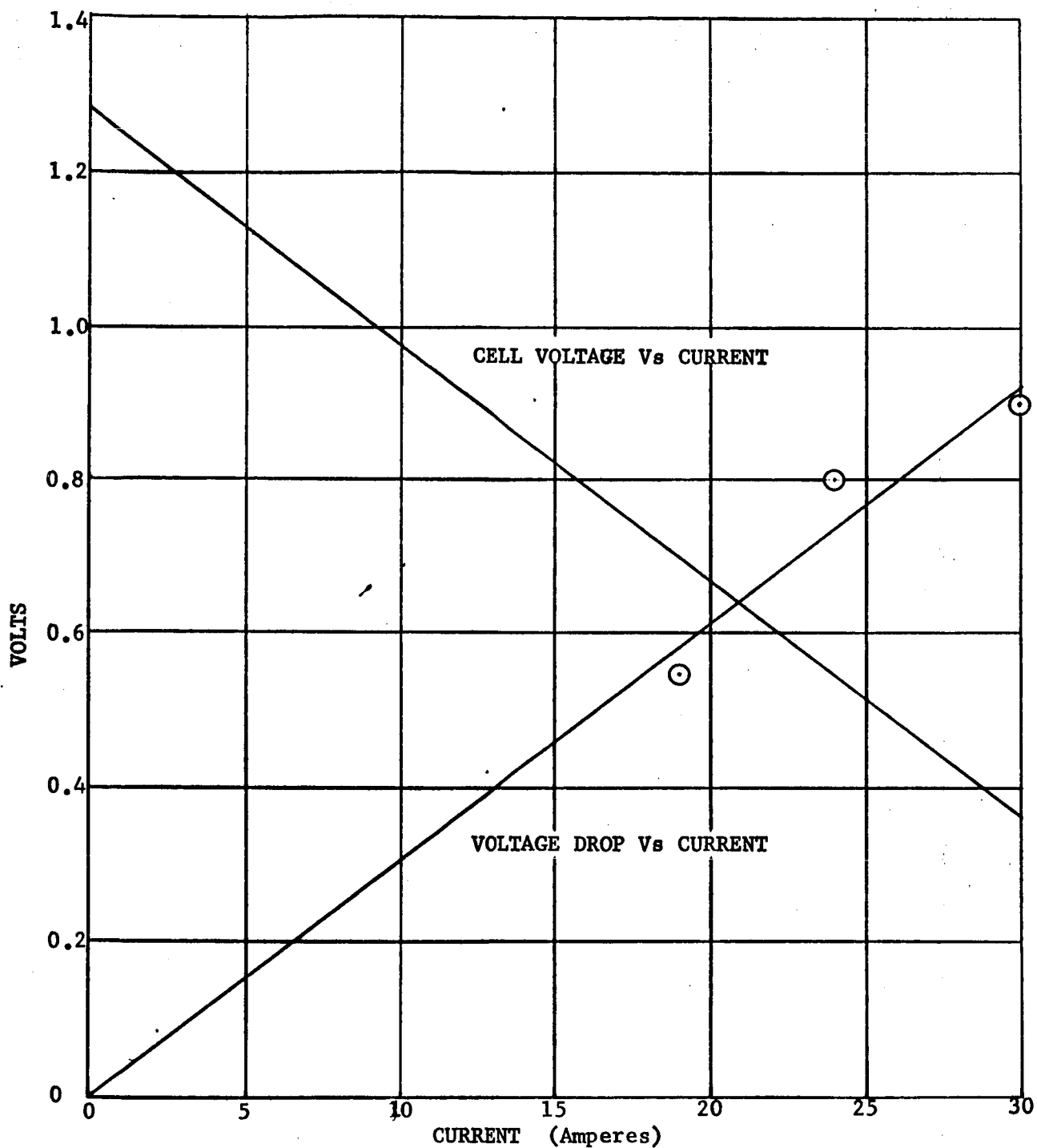


FIGURE 12

VOLTAGE-CURRENT RELATIONSHIP
SINGLE BIPOLAR CELL FOUR IN² ACTIVE AREA
(From Oscilloscope Pictures)

4-1007

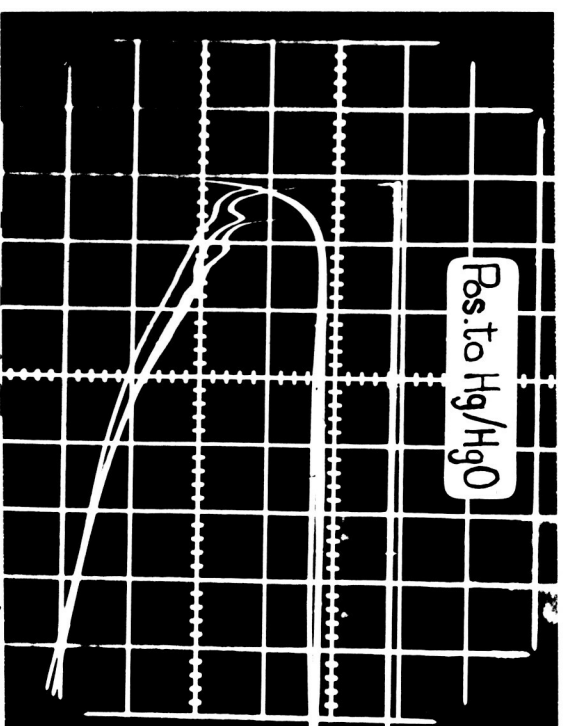
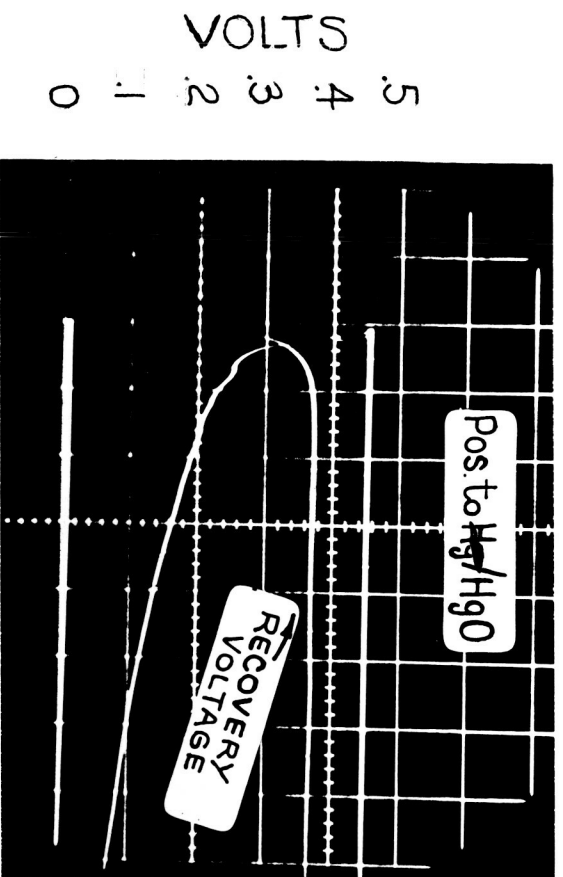
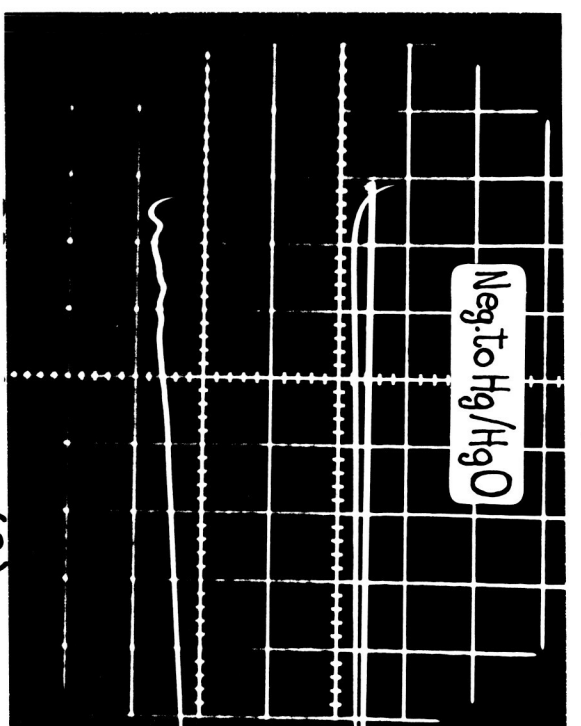
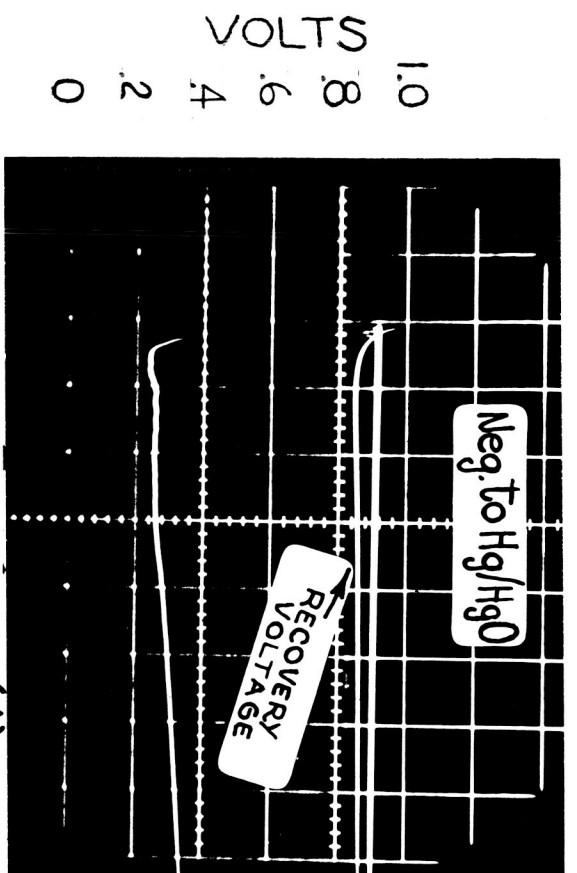


FIGURE 13. ELECTRODE TO REFERENCE PULSES, ALL LOAD AT 0.0244Ω ,
I ~ 24 AMPERES

Single cell pulse discharges were conducted with electrodes having active (sinter) areas of 2.4 in^2 ($1\frac{3}{4}$ inch dia.), 2.7 in^2 ($1\frac{7}{8}$ inch dia.), and 3.1 in^2 (2 in²). The tests were conducted using the forced discharged method at constant current. The results are shown in Figures 14, 15, and 16. The data show an increase in voltage as the active (sinter) areas increase from 2 in^2 to 3.1 in^2 . However, there is a larger jump in performance for the 3.1 in^2 (2 inch dia.) electrodes, although the area increase, in each size, is approximately at a ratio of 1.15:1.

Data from Figure 16 indicate that the 2 in^2 electrode, if assembled into a five-cell battery, would yield 10 amperes at 5 volts. The smaller plates would give marginal performance with respect to the 5 volt cutoff level.

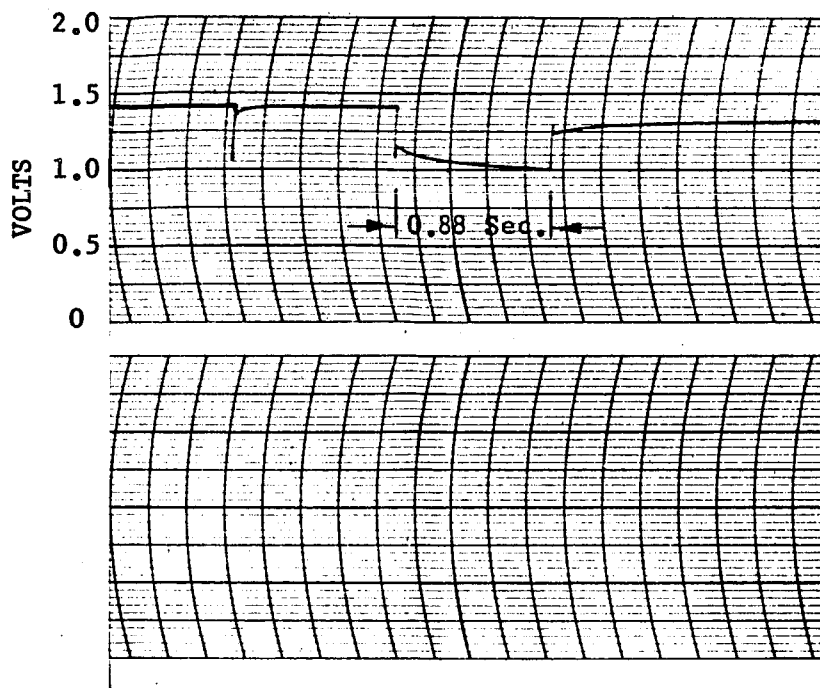


FIGURE 14a PULSE #1 CURRENT 11.0 AMPERES
PULSE DISCHARGE OF A SINGLE BIPOLAR CELL
WITH 2.40 IN² ACTIVE PLATE AREA

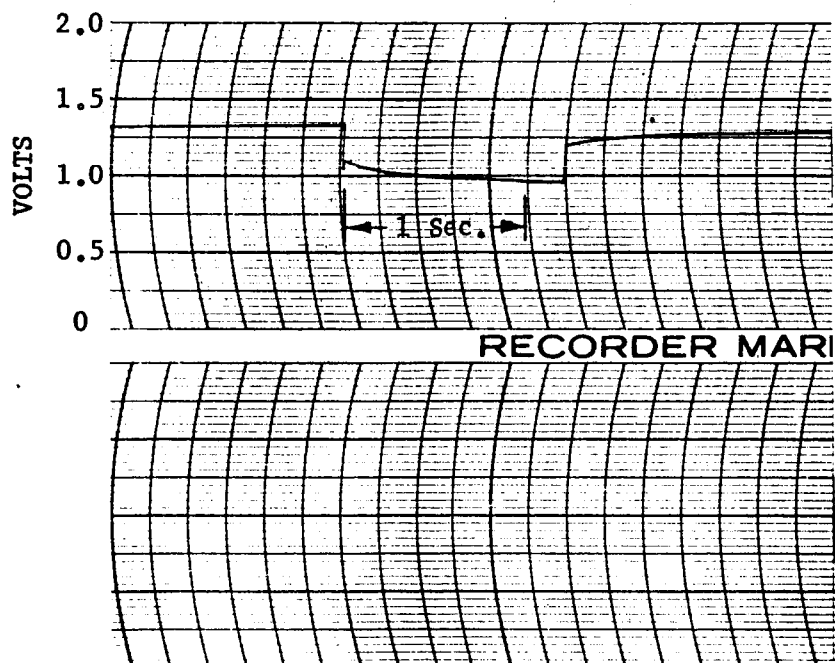


FIGURE 14b PULSE #2 CURRENT 11.0 AMPERES
PULSE DISCHARGE OF A SINGLE BIPOLAR CELL
WITH 2.40 IN² ACTIVE PLATE AREA

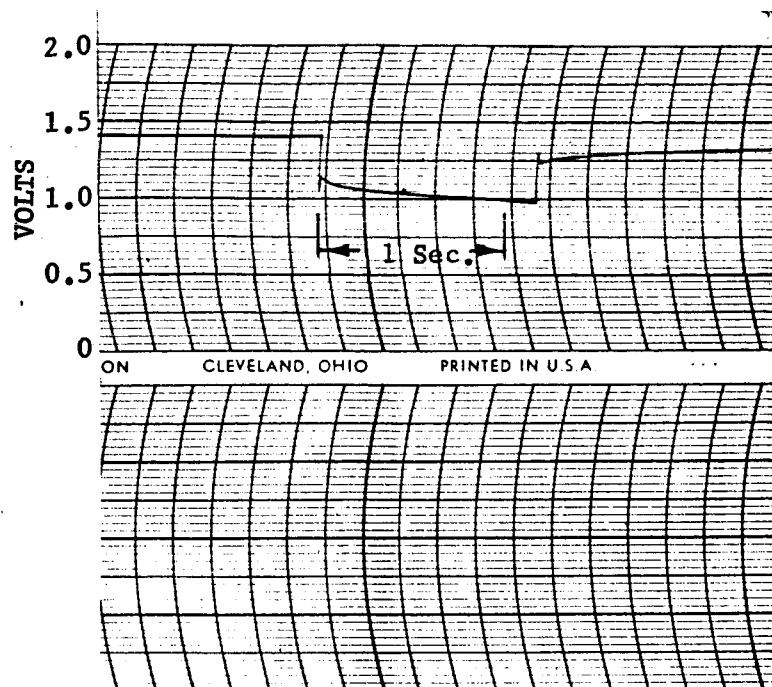


FIGURE 15a PULSE #1 CURRENT 10.5 AMPERES
PULSE DISCHARGE OF A SINGLE BIPOLAR CELL
WITH 2.76 IN² ACTIVE PLATE AREA

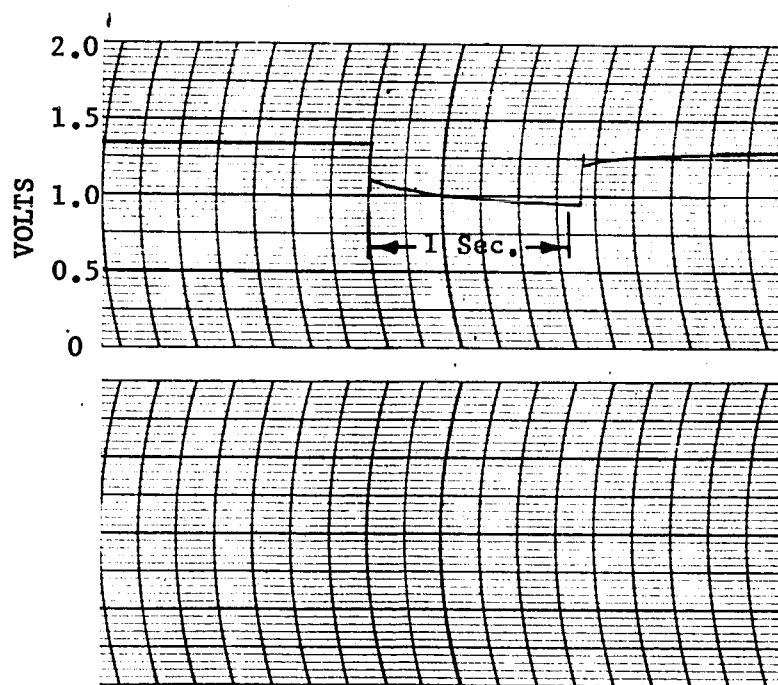


FIGURE 15b PULSE #2 CURRENT 10.5 AMPERES
PULSE DISCHARGE OF A SINGLE BIPOLAR CELL
WITH 2.76 IN² ACTIVE PLATE AREA

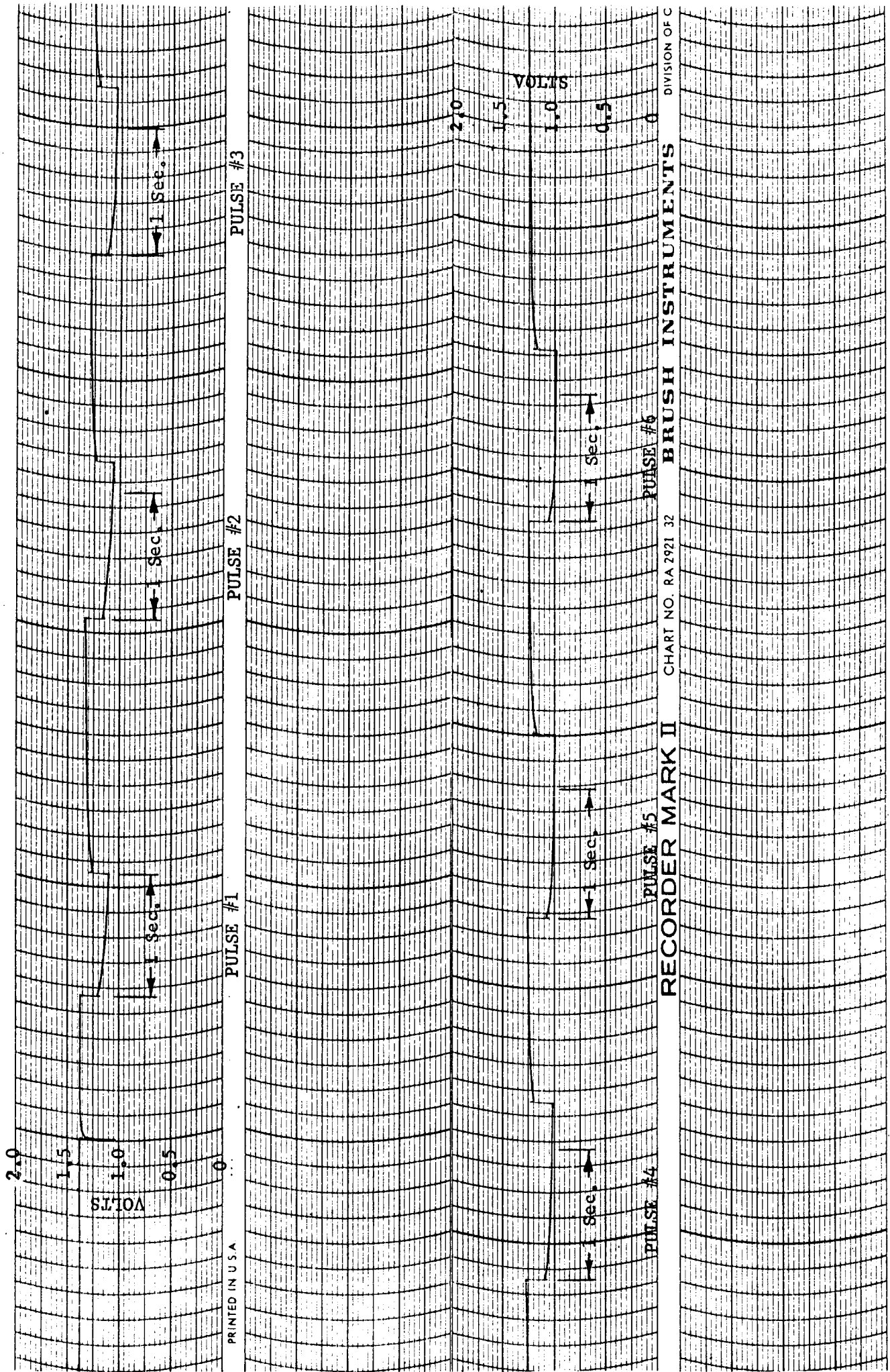


FIGURE 16 PULSE DISCHARGE FOR A SINGLE BIPOLAR CELL WITH 3.14 IN² ACTIVE PLATE AREA
CURRENT 10.5 AMPERES

EVALUATION OF FIVE-CELL BATTERIES

To ascertain the results of single bipolar cells when assembled into five-cell batteries, several were built and tested.

A five-cell battery was assembled from the 1-5/8 diameter electrodes (2 in^2) with a separator of 7 mil non-woven nylon. Sealing the cells was difficult. The battery was assembled in the following manner. The electrode flanges were coated with a sealant (of liquid neoprene) and "O" rings placed between each bipolar plate. The battery was assembled by stacking the plates on top of each other as follows. The electrolyte was added to the sinter, then the separator was placed over the sinter and more electrolyte added. The next bipolar plate was placed on top and the procedure repeated until the end plate was assembled. The battery was clamped between blocks of 1/2 inch thick lucite and fastened with machine screws around the periphery. A photograph of the test battery is shown in Figure 17.

The battery was charged at 10 mA for 27-1/2 hours, with individual cells being monitored. Figure 18 shows the average cell voltage and the spread in cell voltages during the charge. The battery was placed on open circuit with all cell voltages monitored at 1.38 volts. It was then discharged at 100 mA as shown in the right hand side of Figure 18. This figure gives average cell voltages including voltage spread of each cell (battery voltage is five times the average cell voltage). The center cell fell to 0.18 volt after 55 minutes of discharge, although all other cells were at 1.20 volts. After the discharge, the battery was disassembled, the electrodes washed and dried, and reassembled changing the position of the bipolar electrodes. The resultant voltage readings were the same. The center electrode failed first, as before.

A careful study of the situation revealed that the center cell was not sealing and, therefore, losing electrolyte during overcharge; due to the compression method used, the gas pressure during overcharge was forcing electrolyte out. The cell was reassembled using Kel-F grease on the "O" rings. The cell was placed on charge and discharged at the 100 mA rate. All cell voltages were uniform with no visible leaks from the cells. The battery was pulsed at 10 amperes and the voltage recorded on the Brush Recorder Mark II. The results obtained (Figure 19) are almost identical with those shown in Figure 10. The correlation between the 5-cell battery and the single cell of Figure 10 was made by dividing the battery voltage by 5.

A second five-cell bipolar battery was assembled with 4 in^2 (1-3/4 dia.) electrodes. However, to give the cells additional free volume, and to compensate for the effects of concentration polarization, the negative side of the sinter was cut down to 1-5/8 inch diameter (2 in^2). This gave the battery an active area of 2 in^2 . Each cell had a free volume equal to the difference of the positive electrode (2.40 in^2) and negative electrode (2.07 in^2), times the thickness of one electrode (.030 inch), or approximately 0.16 cc.

An elastometer type seal known as "Quad-Ring Seal", manufactured by the Minnesota Rubber Co., Minneapolis, Minnesota, was used to seal individual cells of the battery. This seal makes a two point contact with a sealing surface. The relative square cross-section of the "quad" ring and flexibility of the four-lobed sealing surface, made it easier to apply

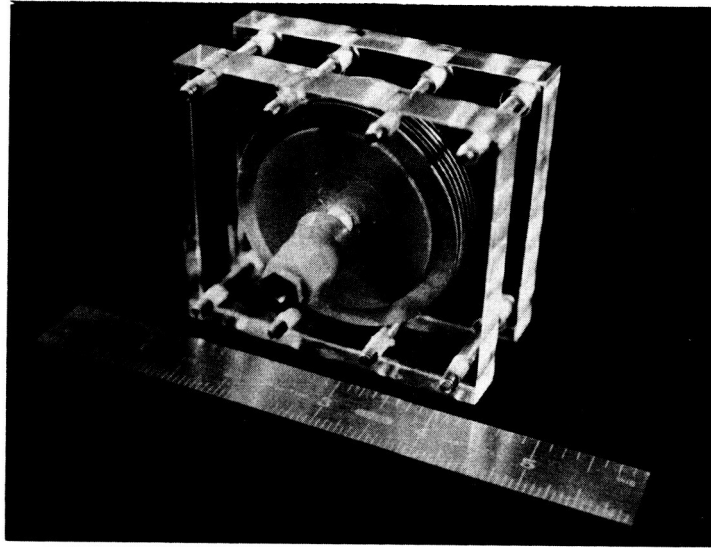


FIGURE 17. FIVE CELL BATTERY WITH 2 IN² OF SINTER AREA

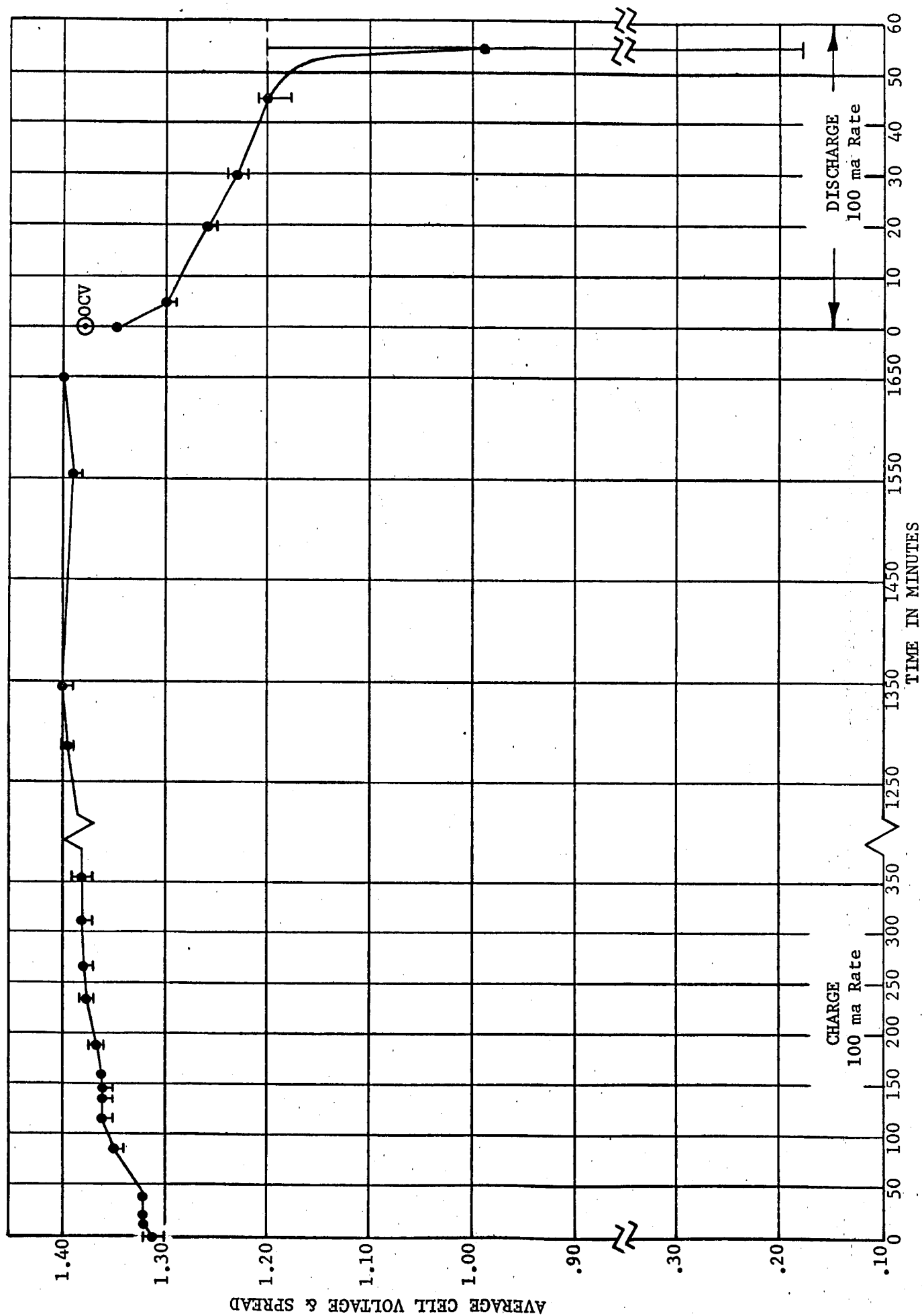


FIGURE 18 CHARGE & DISCHARGE OF A 5 CELL BATTERY SHOWING AVERAGE CELL VOLTAGE & SPREAD

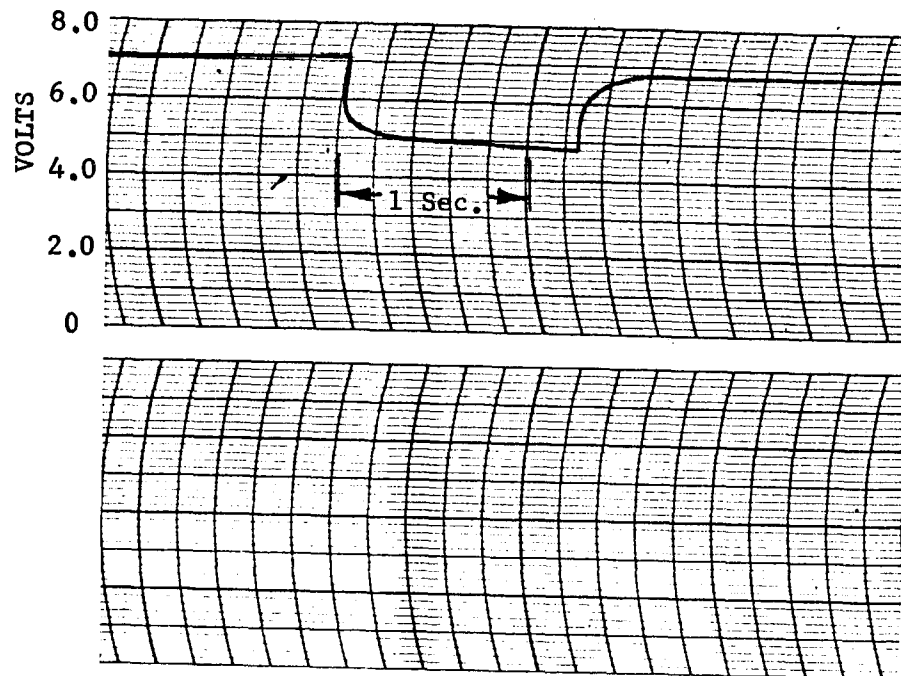


FIGURE 19a

PULSE NO. 1 CURRENT 10 AMPERES
PULSE DISCHARGE FOR A 3 CELL BIPOLAR BATTERY
WITH ACTIVE PLATE AREA OF 2.07 IN^2 / PLATE

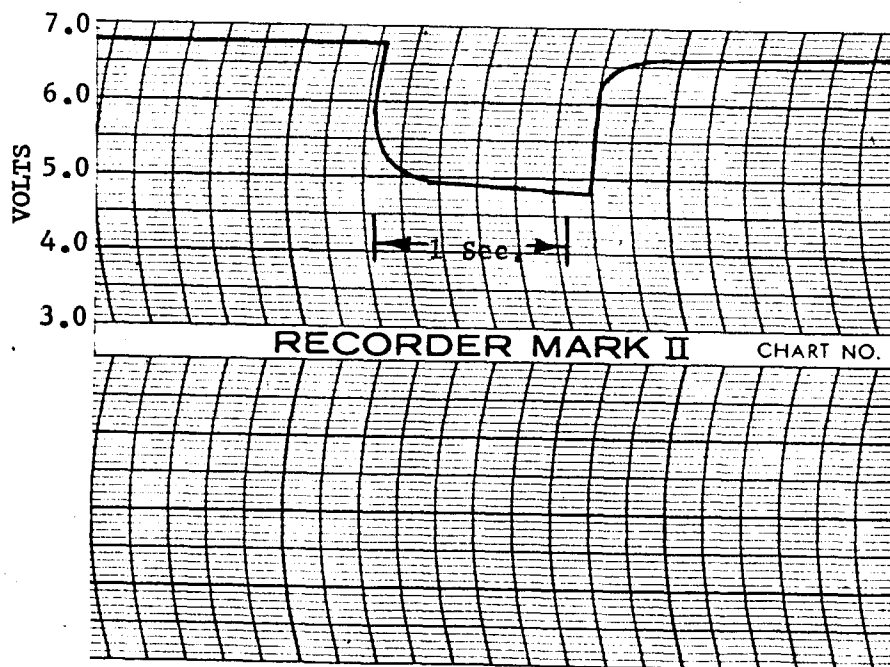


FIGURE 19b

PULSE NO. 2 CURRENT 10 AMPERES
PULSE DISCHARGE FOR A 5 CELL BIPOLAR BATTERY
WITH ACTIVE PLATE AREA OF 2.07 IN^2 / PLATE

pressure to the cell stack and obtain intimate contact between wet separators and electrodes, for lower cell impedance. A cross-sectional view of a single bipolar cell assembled with a "quad" ring is shown in Figure 20.

The five-cell battery (2 in^2 active area) was encapsulated in a potting compound with positive and negative threaded terminals protruding from it. After one formation cycle, the battery was pulsed across a 0.49 ohm load for six consecutive one second pulses. The results are shown in Figure 21. These results are identical with those previously obtained from five-cell, 2 in^2 , bipolar batteries. The voltage on the first pulse was 4.9 volts.

Following the pulse discharges, the battery was given a constant current charge of 15 milliamperes. After sixteen hours of charging, a small electrolyte leak was observed emanating from the junction of the positive stud and potting compound. The battery was taken apart and examined for causes of failure. It was found that the leak occurred from one cell, the end cell, where the electrolyte had penetrated the bond between the potting compound and the end plate.

A third five-cell battery was assembled. The electrode sizes of both the positive and negative sinters were $2\text{-}1/4"$ in diameter (4 in^2 of active area). The nickel substrates were thoroughly cleaned, sand blasted, wiped down with MEK, and washed and dried. The electrolyte was introduced into each cell prior to assembly by wetting the 7 mil, non-woven nylon separator with KOH and wetting the sinters with the balance until it was all absorbed. The edges of the nickel substrate were again cleaned with a mild solution of boric acid, washed and dried. A "quad" ring, coated thinly with Kel-F grease, was placed between each cell. The entire 5-cell module was then placed into a tightly held mold and encapsulated with a potting compound, ERL-2795, manufactured by Union Carbide Co. After the potting compound solidified, the battery was removed from the mold and restrained between two lucite sheets, $1/2$ inch thick, and placed on charge at the 20 mA constant current rate.

Prior to pulsing at the 10 ampere rate, the battery was given one discharge at 600 mA to one volt. The capacity above 1.0 volt was 570 mAh.

The battery was given a second charge and pulsed at 10 A for one second. The voltage and current were recorded on an oscilloscope. The oscilloscope traces of the pulse discharge are shown in Figure 22.

The voltage at the 10 ampere pulse was at the 5 volt level for the large 4 in^2 bipolar battery.

It was felt that, even though no leaks were immediately observed, this method of sealing offers no measure of reliability, and other techniques need to be developed to obtain a reliable seal.

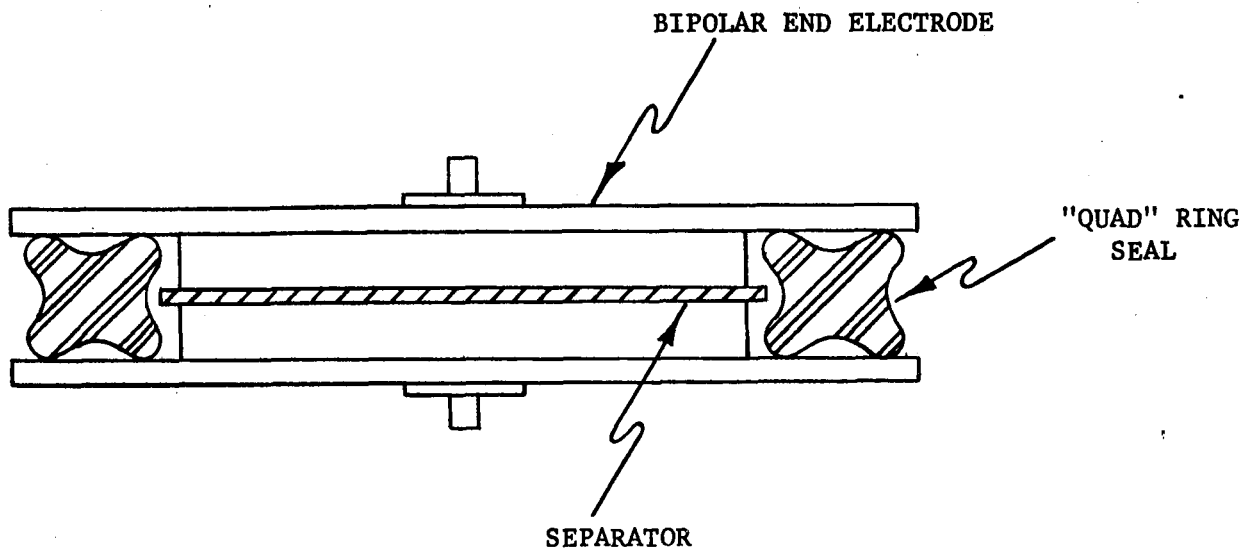


FIGURE 20 CROSS-SECTIONAL VIEW OF A BIPOLAR CELL
ASSEMBLED WITH A "QUAD" RING SEAL

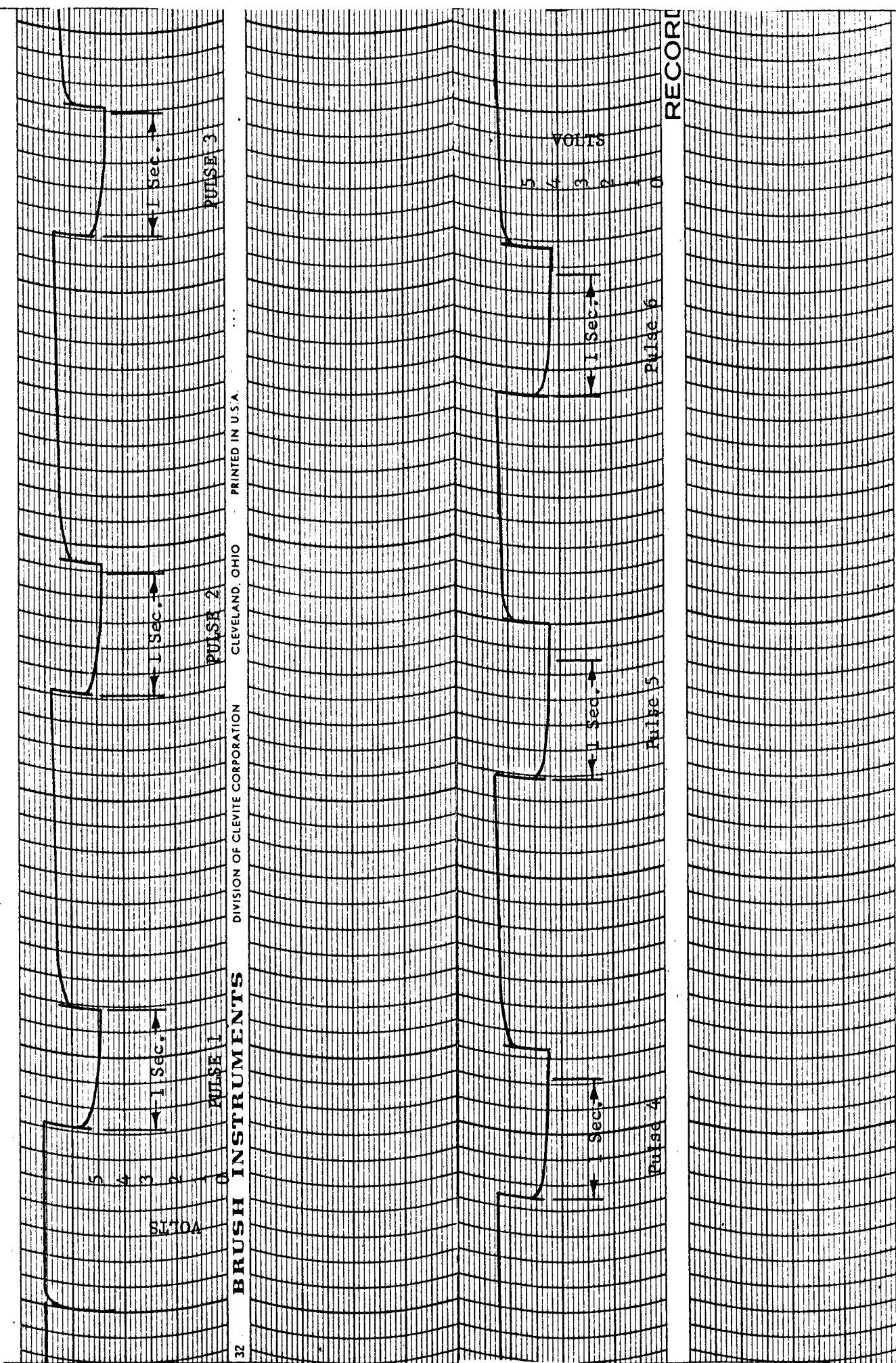


FIGURE 21 PULSE DISCHARGES FOR A 5 CELL BIPOLAR BATTERY WITH 2.40 IN² POSITIVE AND 2.07 IN² NEGATIVE ACTIVE PLATE AREAS

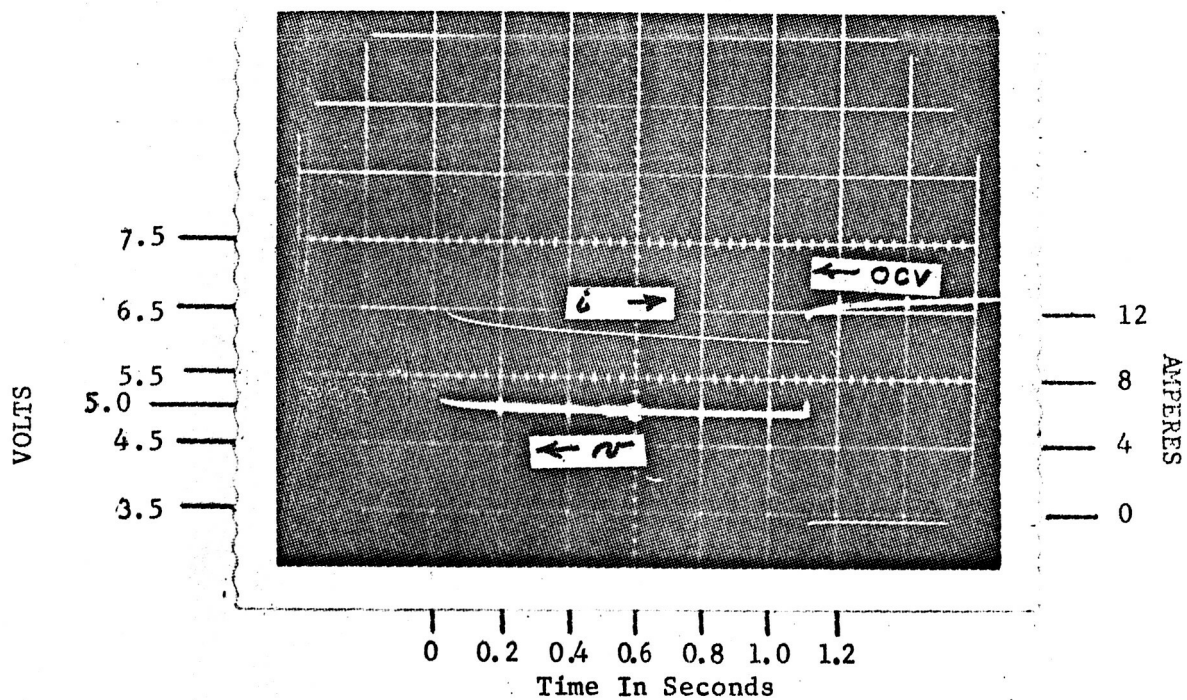


FIGURE 22 OSCILLOSCOPE TRACES FOR A PULSE DISCHARGE OF A 5 CELL, 4 IN² BIPOLAR BATTERY

Adhesive Bonding

The application of a rubber-to-metal adhesive bond in the assembly of bipolar batteries suggested itself when other means failed to produce reliable seals.

The joint geometry is particularly adaptable for adhesive bonding since the substrate is an ideal lap joint in tension with the stress (generated by the cell pressure) perpendicular to the plane of the joined surfaces.

With proper assembly techniques, cleavage and peel stresses can be minimized. The added support of the encapsulating compound would contribute to uniformity of stress distribution across the adhesive joints and prevent peeling tendencies caused by the tensile stresses in the free edges of the adhesive joints.

Surface Treatment

An important aspect of adhesive bonding is the surface preparation and treatment prior to making the joint. Adherent surfaces must be pretreated and kept clean until bonded.

Although the forces which produce adhesion between organic materials and metal surfaces are not clearly understood, it is known that these forces are short-range with respect to molecular dimensions. Therefore, the presence of foreign substances will interfere with the close approach or intimate contact between adhesive and adherent, and would result in lower surface energy and poor bond.

Three methods for cleaning the surface of the nickel substrate were considered: chemical, mechanical abrasion, and degreasing. With some variations in procedures, the latter two were employed. The chemical cleaning was not considered practical. The recommended composition of the etchant for nickel is a strong concentration of nitric acid. This was not considered practical in view of the fact that bipolar electrodes were fully impregnated, and the presence of acid in the sinter could not be tolerated nor effectively neutralized.

A flow chart of the cleaning methods used, and found to be practical for this application, is shown in Figure 23.

Sand blasting was considered the most practical method of mechanical abrasion. The electrodes were placed in a fixture, masking the sinters and only the bonding edges were exposed to the abrasives. A uniform surface roughness was thus obtained. The roughness factor of the nickel substrate was considered to be significant in obtaining a good joint. A uniformly roughened surface will possess a larger actual area for the action of molecular forces. The roughening is usually accompanied by an increase in the free surface energy produced through working of the surface and through the higher surface energy property possessed by rough metal crystals.

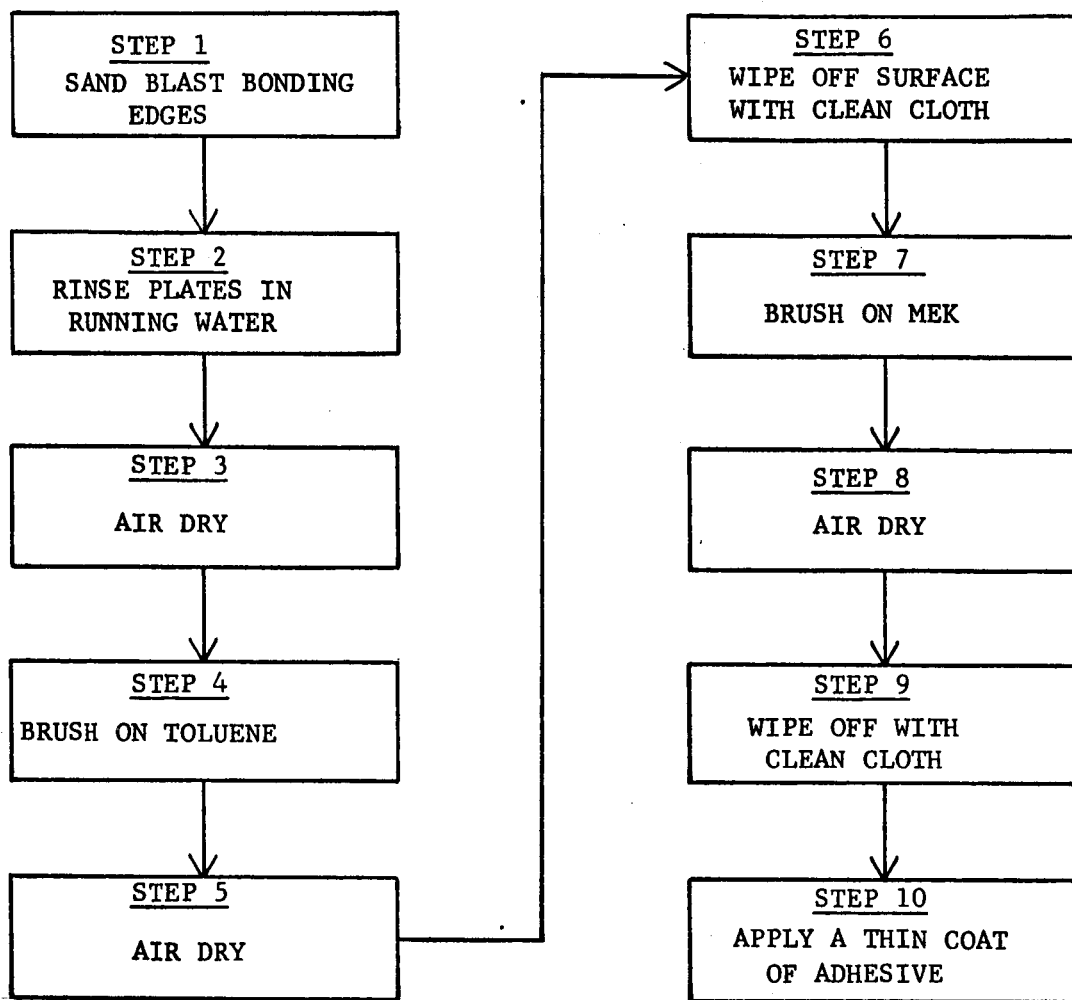


FIGURE 23 FLOW CHART FOR SURFACE PREPARATION OF NICKEL SUBSTRATES FOR BIPOLAR BATTERIES

To test the surface for proper preparation and cleanliness, each electrode was given the "water break" test. A droplet of distilled water was placed on the cleaned surface and observed to see if it spread and wet the surface smoothly. It was felt that if a drop of distilled water wets the metal surface and spreads smoothly over the surface without breaking up into individual droplets, the surface could be presumed to be free of harmful organic films. A surface which is uniformly wet by distilled water will probably also be wet by the adhesive. The surfaces were thoroughly dried after each test.

Adhesives and Seal

Several known organic compounds were tested as a rubber-to-metal adhesive. The adhesives that were recommended for bonding nickel-base alloys are in a class known as thermosetting adhesives. These undergo chemical changes during the curing cycle and effect a bond between the rubber and metal. The adhesive sought for this application, initially, was one requiring the minimum curing temperature. Since the electrodes to be bonded are impregnated with active materials, adhesives with room temperature curing cycles were sought, to minimize the heat effect on the active materials and cell function.

A list of bonding agents, curing at room temperature, was tested and evaluated. In each case, the bond failed to hold up when subjected to KOH environment. It was apparent that reliable bonds to nickel could not be achieved with the room temperature curing adhesives and that thermosetting adhesives would have to be adopted.

The major problem was to localize the heat around the flange and to limit the temperature for the entire electrode to 300°F.

A combination of primer and adhesive, which cure at 300°F was finally used. The primer was applied to a cleaned and conditioned nickel substrate and allowed to air dry to vaporize the solvents which are commonly found in adhesives. In many samples, the presence of solvents in the adhesive and their inability to escape from the bonding surfaces, resulted in extended cure time and porous bonds.

The rubber seal used to bond to the surface was a cured neoprene washer, 45-55 durometer, manufactured to Spec. MIL-R-3065. The gasket was soaked in the adhesive and placed over the primed surfaces of the substrate.

The assembly was clamped between two rings and placed into a hydraulic press with heated elements. The temperature was maintained at 300°F for one hour on the pressure rings. The bonded half-plates were assembled into a bipolar cell by flooding the inside with KOH. The rubber-to-rubber bond between the cell halves was accomplished using a neoprene cement. A cross-sectional view of the cell is shown in Figure 24.

The test cell was subjected to temperature cycling between 73°F and 150°F for 32 hours, after which the cell was placed on the shelf for 2 weeks. At the end of this period, the cell showed no signs of leaking. The cell was taken apart by prying open the seal. There was evidence of interface attack and a joint weakening at the interface of the rubber and metal.

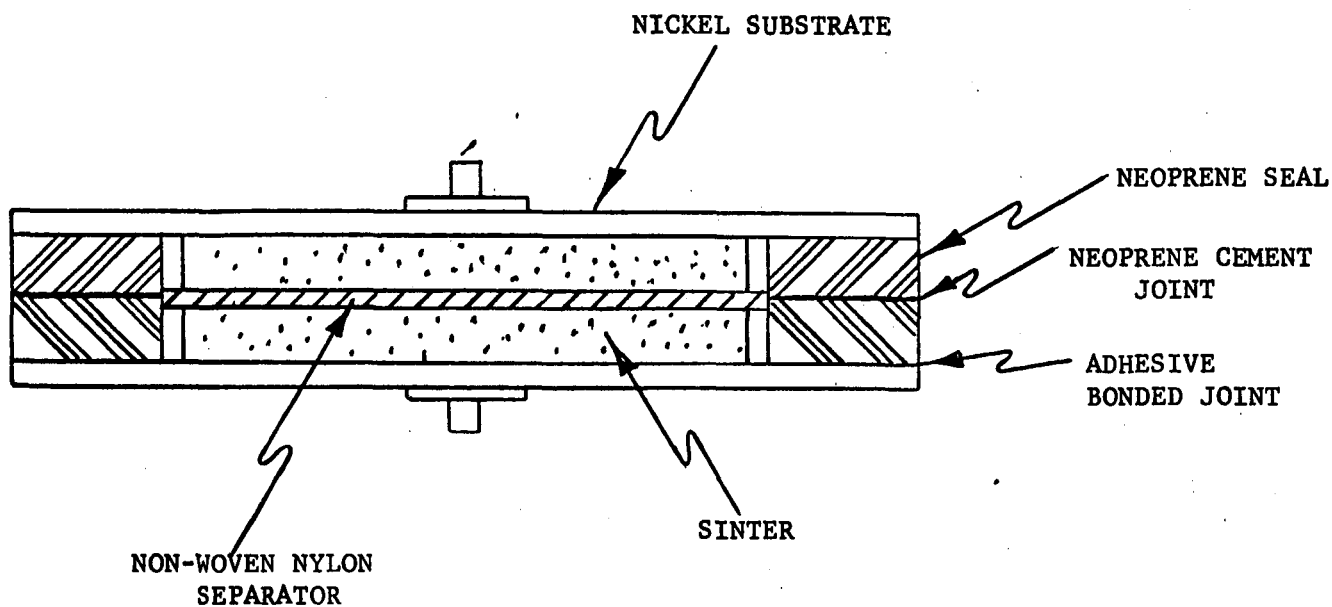


FIGURE 24 CROSS-SECTIONAL VIEW OF A RUBBER-TO-METAL
SEAL IN A BIPOLAR CELL

THE SEAL WAS CURED NEOPRENE

In a parallel test program, several cells and two 5-cell batteries, with 2-1/4 inch diameter sinter area, were built using uncured neoprene, 40 durometer, in lieu of the cured neoprene washers, and the same bonding adhesive which was applied to the cleaned and conditioned nickel substrate and air dried. The uncured neoprene was placed on both parts of a set of matching steel molds and applied over both substrate edges of the bipolar electrode. The entire package was placed in a hydraulic press with heated elements and maintained at a temperature of 300°F and 1500 lb/in² of pressure. A photograph of the press is shown in Figure 25.

Upon air cooling, the edges of the electrode were trimmed of the excess neoprene, and the electrode was ready for assembly, as previously described. Figure 26 shows a half mold for vulcanizing seals.

The bonds obtained between the rubber and the metal during vulcanization have been tested and found to be superior to those previously obtained without vulcanizing.

The bonded 5-cell module was then encapsulated in a potting compound. The batteries so assembled, showed no trace of leakage when subjected to normal cycling. Subsequent destructive tests showed that the bonds were stronger than the rubber when subjected to peel and tensile tests. Cells subjected to simulated cell environment held up well with no signs of bond weakening.

Assembly Procedures and Test Results of 10 Development Batteries

The quantity of electrolyte in a sealed nickel-cadmium cell must be closely controlled for optimum cell performance. The internal volume available in each bipolar cell (2 to 4 in²) is small. Hence variations in electrolyte quantities, even in the hundredths of a cc, are relatively large as a percentage of the total. It was difficult to determine the exact quantity of electrolyte needed for each cell of each size, and therefore, vented formation of flooded cells was used.

Cellulosic separators, 3 mil thick, were used in lieu of non-woven nylon. The cellulosic separators swelled on soaking in electrolyte and made intimate contact with both electrodes. This condition prevented any void space between the electrodes and gave a full cross section for current carrying. Five-cell bipolar modules, similarly assembled, using non-woven nylon separators, showed a tendency to form "hot spots" (places where, due to the electrolyte forming a local path, the current followed a path of least resistance) and the apparent internal resistance went up. Voids, created inside the cell due to poor separator contact between the electrodes, reduced the electrode surface area and, therefore, operated at higher current densities than calculated.

Five-cell modules were assembled dry, with the rubber bonded seals, and were then filled with electrolyte (flooded) through protruding filling tubes. They were then subjected to a vented formation regime. The vented formation procedure permitted a high rate overcharge (C/4 for five hours), which more efficiently reactivated the nickel and cadmium electrodes. Such high rate charge of a sealed cell would result in excessive pressure build-up and probable failure of the seal.

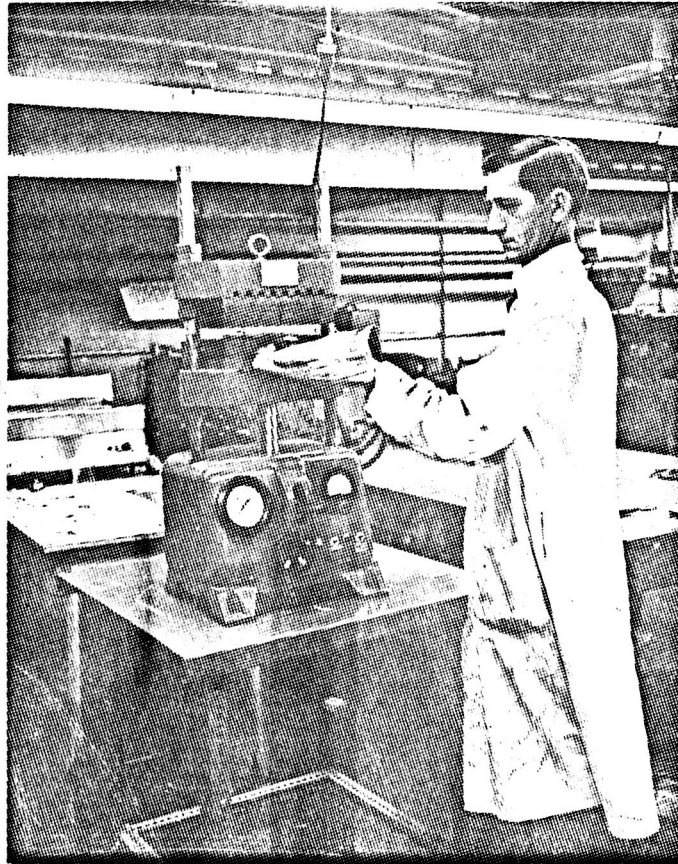


FIGURE 25

WABASH PRESS WITH HEATED PLATTENS FOR
VULCANIZING RUBBER SEALS

OPERATOR LOADING ELECTRODES

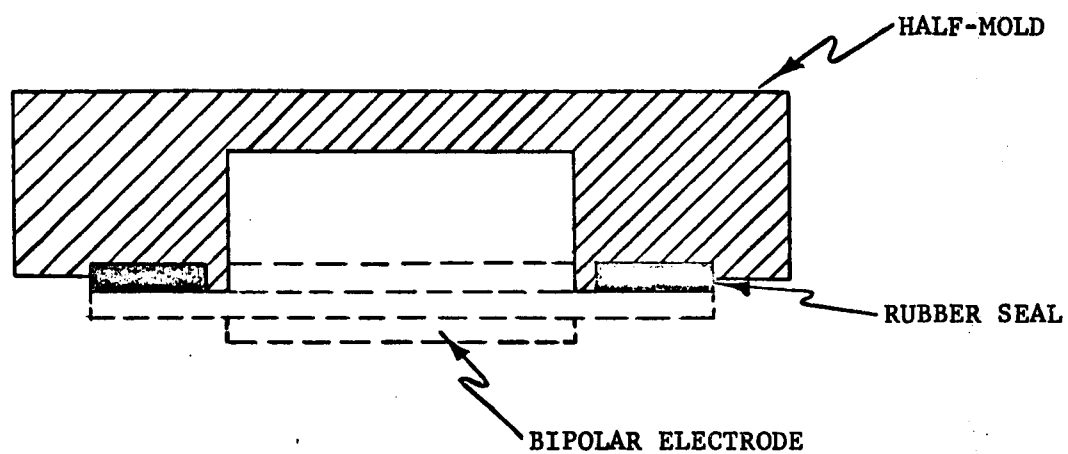


FIGURE 26 HALF-MOLD FOR VULCANIZING RUBBER SEAL
TO SUBSTRATE OF BIPOLAR ELECTRODE

Figure 27 shows oscilloscope traces for 8 consecutive pulse discharges of a five-cell vented module--3.1 square inches of active area. The voltage on the first five cycles is above 5 volts with the current in excess of 10 amperes.

Figure 28 shows oscilloscope traces of two consecutive pulse discharges of a five-cell vented module with 2.76 square inches of active area. The current, on the first pulse, is above 11 amperes with a voltage of 5.4 volts.

After the first formation cycle discharge, the battery, vented, was fully charged. It was then inverted (with the filling tubes facing downward) and the excess electrolyte spilled out. The filling tubes were removed and the openings sealed with a neoprene cement.

The five-cell modules (sealed and flooded) were restrained between two 1/2 inch lucite plates and subjected to ten, one second pulse discharges (battery position was random since it can operate in all positions). Oscilloscope traces of 13 consecutive discharges of a sealed, five-cell module with 3.1 in² of active area, are shown in Figures 29a through 29f. The first 10 pulses were repeated at one second intervals, while the last three were at two minute intervals. The voltage on the first three pulses was approximately 5.5 volts and the current 11 amperes. The voltage stays above 5 volts at the fifth pulse, and gradually declines slightly below the five volt limit. After two minute intervals, the voltage recovers to 5 volts at 10 amperes on the next three pulses. Figure 30 shows similar data for a sealed, five-cell module with 2.76 in² of active area.

After the pulse discharges (ten pulses), individual cells of the battery (through the exposed nickel edges of the substrates) were drained at 150 mA to approximately 0.6 volt per cell. The rubber surfaces were thoroughly cleaned and air dried. The sealed, five-cell modules were placed in a plastic mold and encapsulated in a potting compound leaving the two end terminals exposed.

Figure 31 shows a photograph of a five-cell, sealed module, 3.1 in², encapsulated.

The compound, in this case, served as a convenient means for packaging the module and as a dielectric material separating bipolar cells from each other. Mechanical packaging of modules inside metallic or plastic containers for retaining the modules, prevent expansion of the stack which increases the apparent internal resistance during charge and discharge, were not considered and were felt to be outside the scope of this program.

After encapsulation, the five-cell modules were allowed to harden in the mold. They were then removed and charged at a constant current, in the following manner: 25 milliamperes per square inch of active plate area (80 mA for a 3.1 in² electrode) until the voltage reached 7.1 volts for a five-cell battery (1.42 volts per cell); the current was then reduced to 15 mA per square inch until the voltage again reached 7.1 volts. A third step in charging was used when the total input was considered insufficient. In this case, the current was reduced to 12 mA/in² until the voltage again reached 7.1 volts.

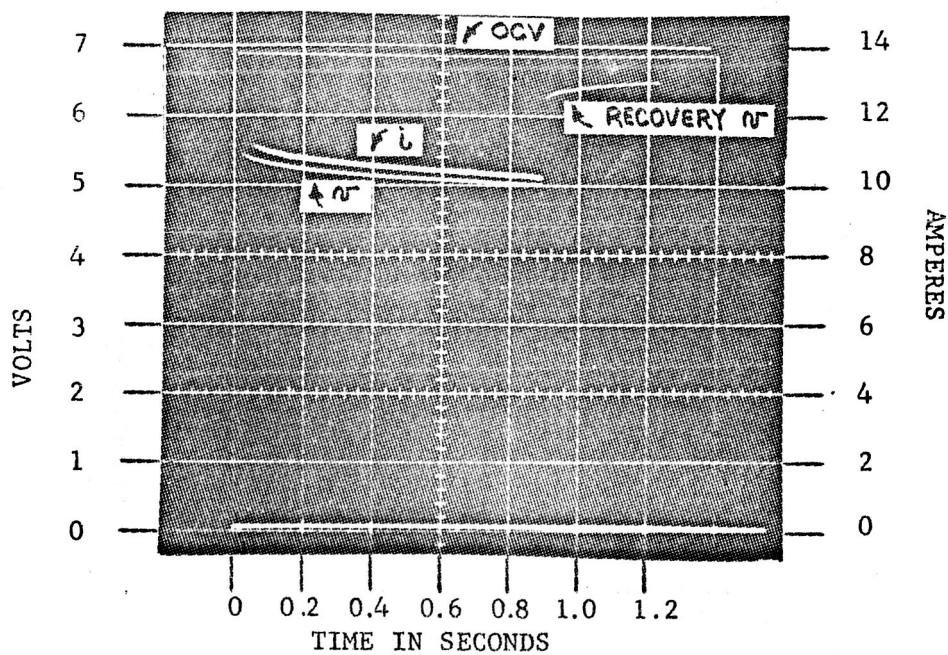


FIGURE 27a PULSE NO. 1

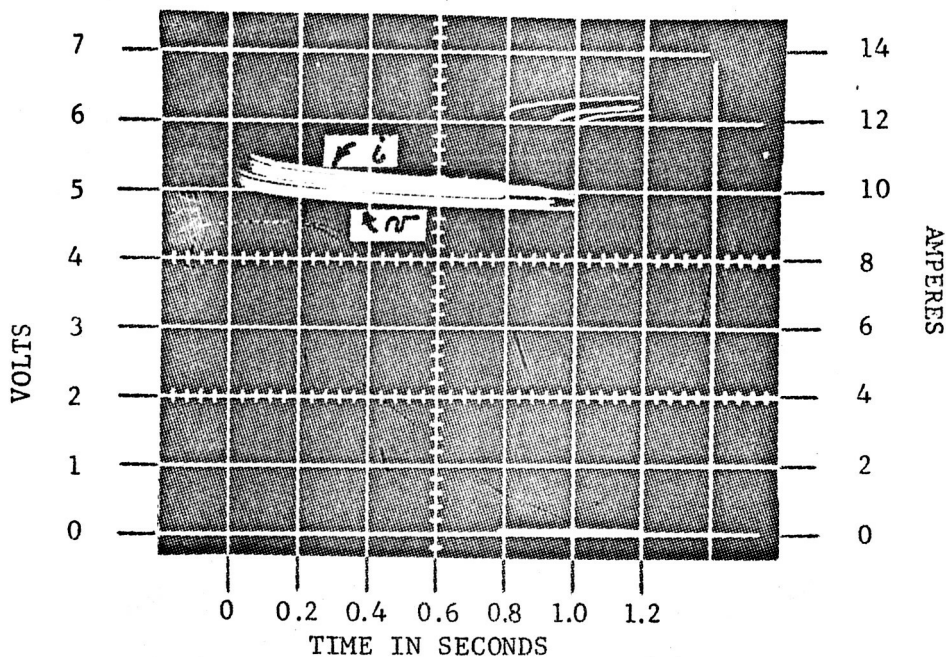


FIGURE 27b PULSES NO. 3, 5 7, & 8

OSCILLOSCOPE TRACES FOR 8 CONSECUTIVE PULSE DISCHARGES
OF A FIVE-CELL, VENTED, 3.1 IN² BIPOLAR BATTERY

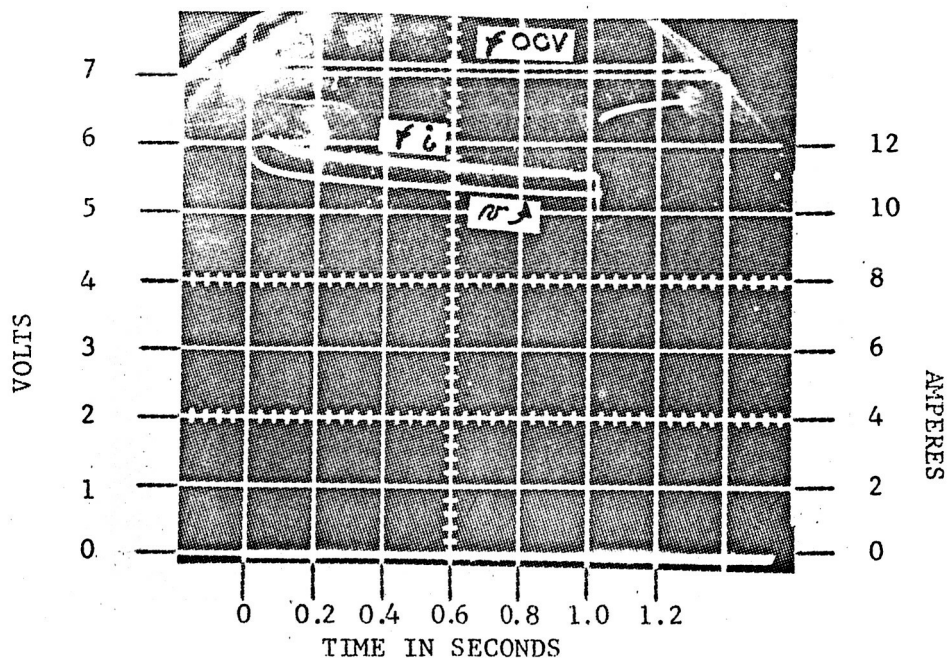


FIGURE 28a

PULSE NO. 1

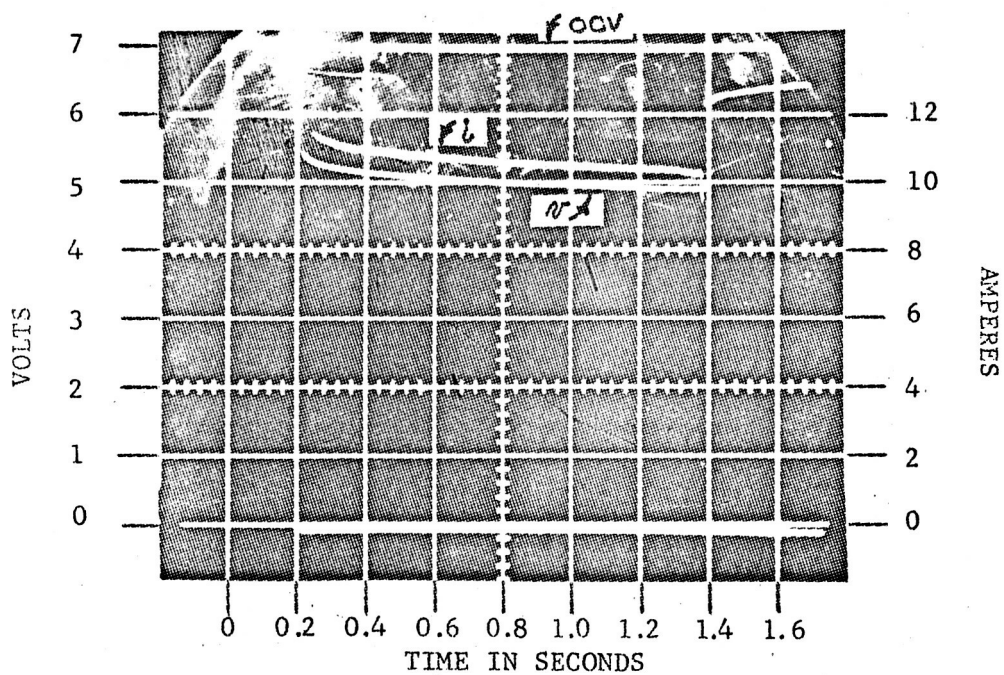


FIGURE 28b

PULSE NO. 2

OSCILLOSCOPE TRACES FOR 2 CONSECUTIVE PULSE DISCHARGES OF
A FIVE-CELL, VENTED, 2.76 IN² BIPOLAR BATTERY

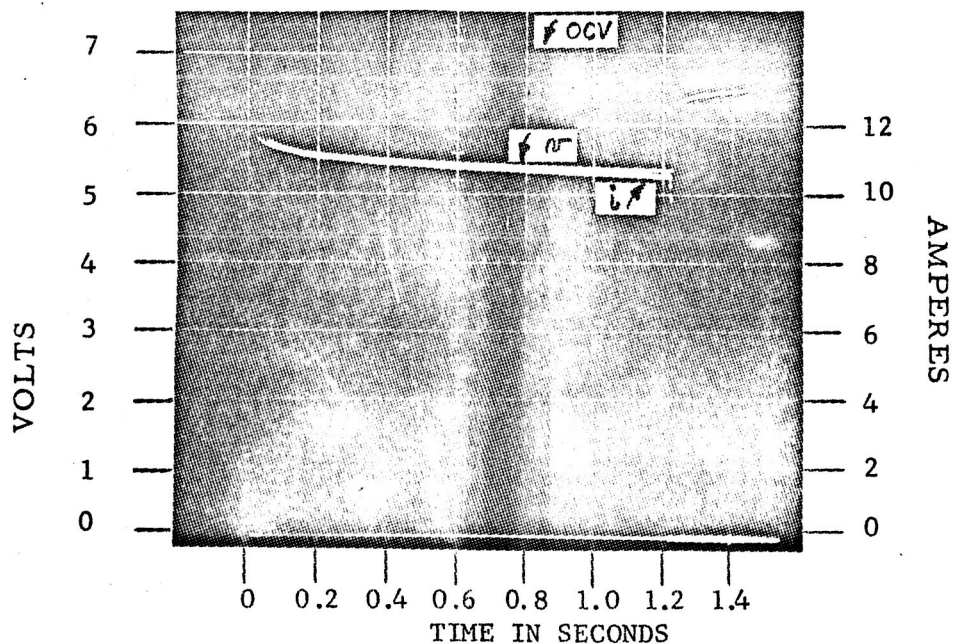


FIGURE 29a

PULSE NO. 1

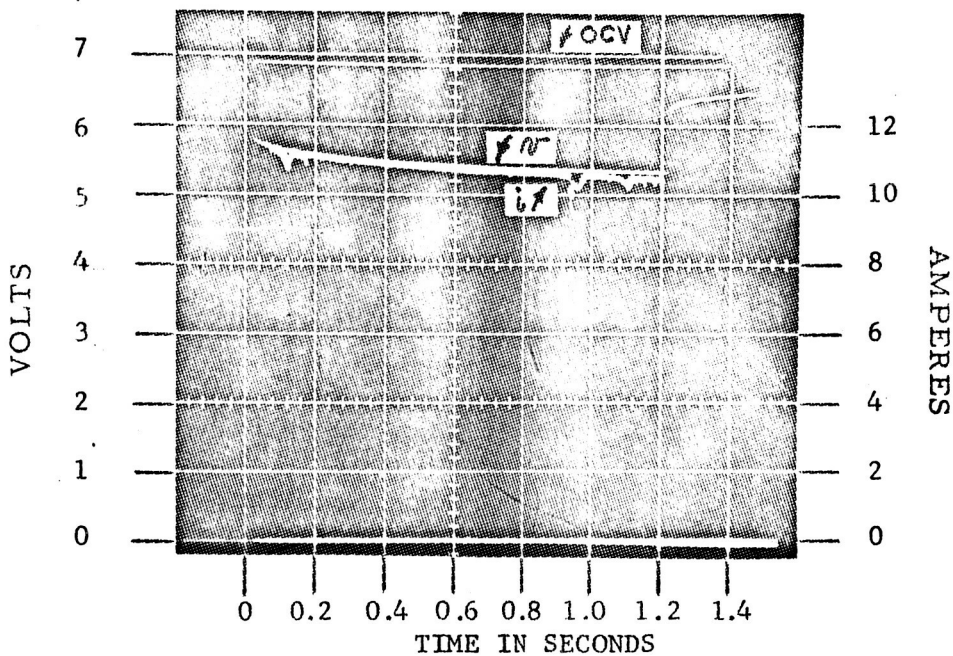


FIGURE 29b

PULSE NO. 2

OSCILLOSCOPE TRACES FOR 13 CONSECUTIVE PULSE DISCHARGES
OF A 5-CELL, SEALED, 3.1 IN² BIPOLAR BATTERY

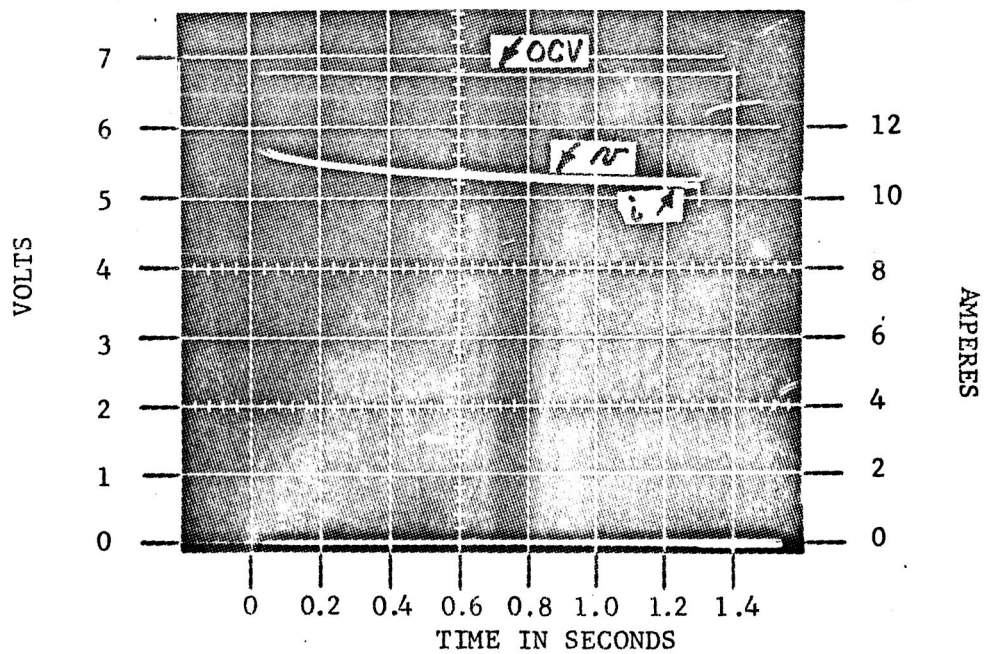


FIGURE 29c

PULSE NO. 3

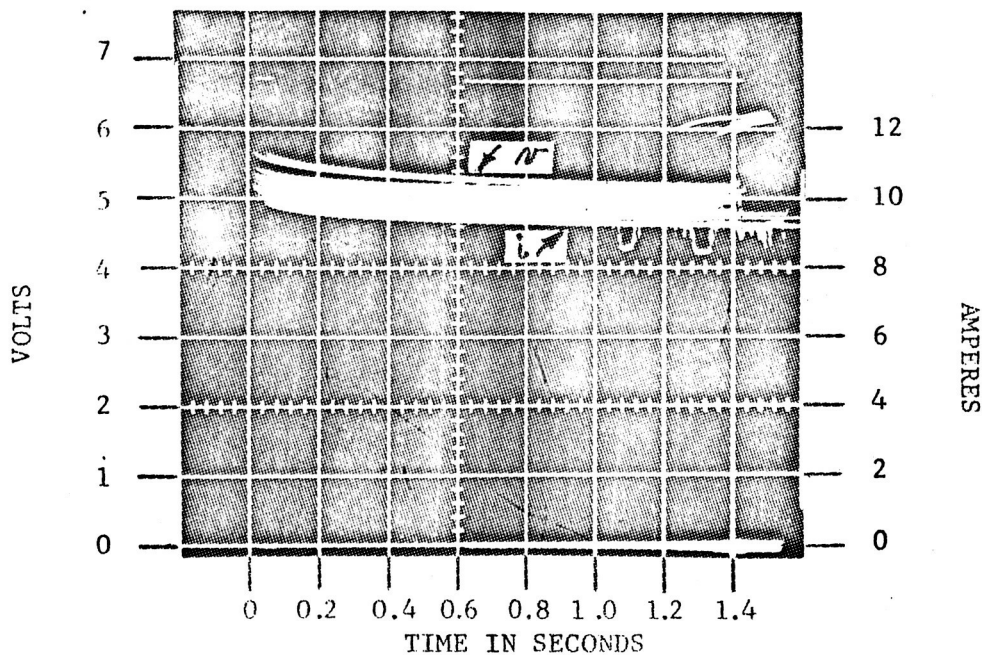


FIGURE 29d

PULSE NOS. 4 THRU 10

OSCILLOSCOPE TRACES FOR 13 CONSECUTIVE PULSE DISCHARGES
OF A 5-CELL, SEALED, 3.1 IN² BIPOLAR BATTERY

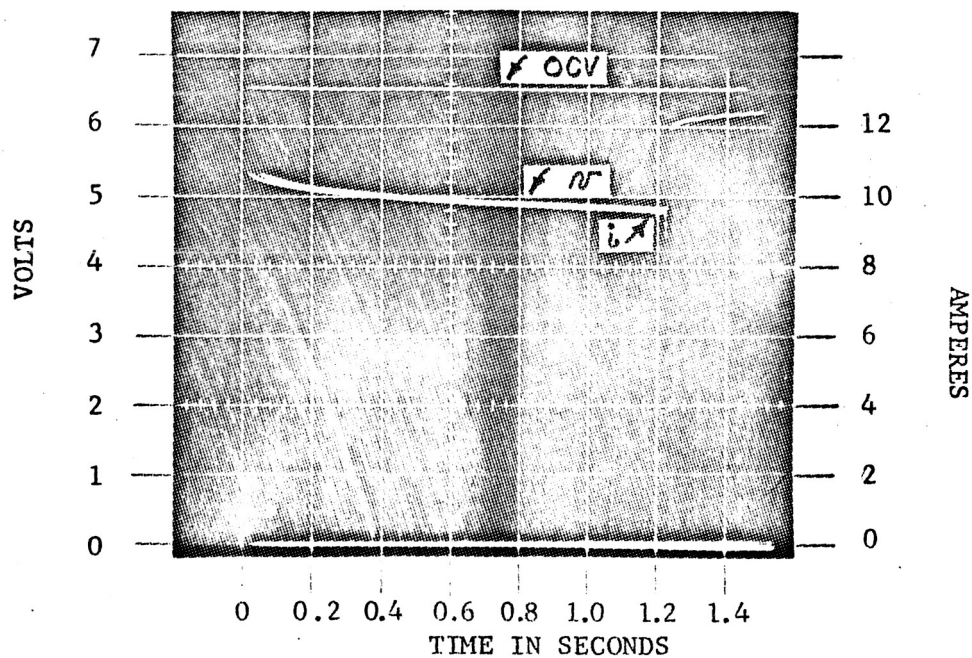


FIGURE 29e

PULSE NO. 11

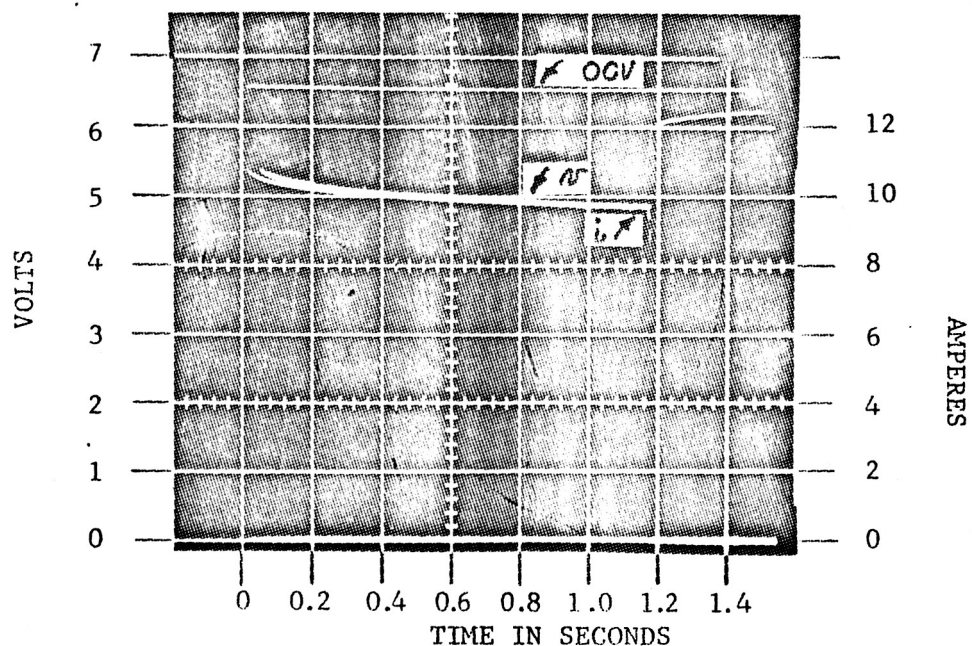


FIGURE 29f

PULSE NO. 13

OSCILLOSCOPE TRACES FOR 13 CONSECUTIVE PULSE DISCHARGES
OF A 5-CELL, SEALED, 3.1 IN² BIPOLAR BATTERY

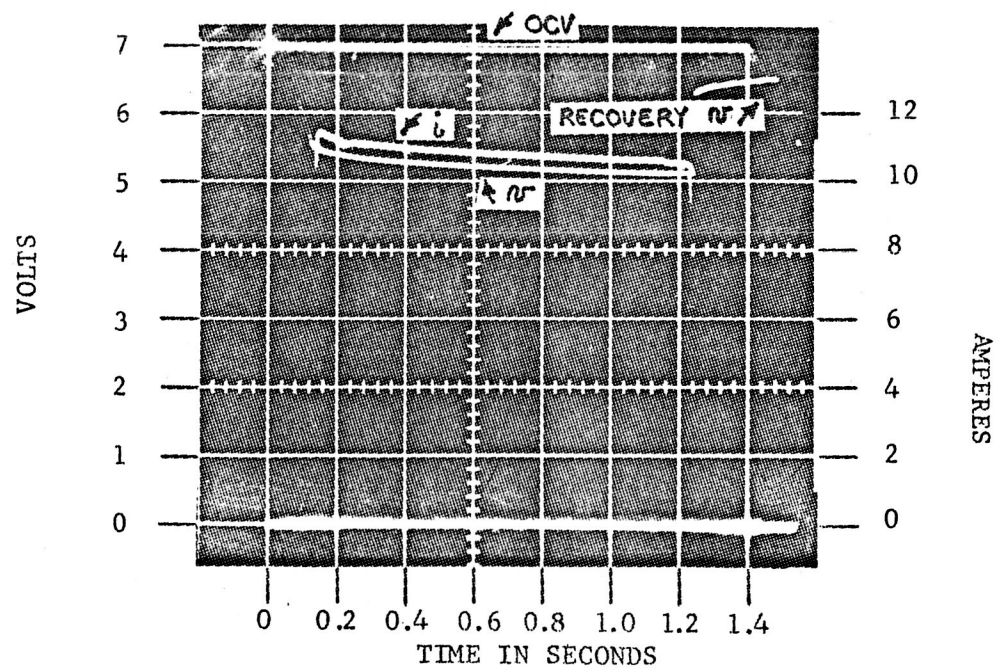


FIGURE 30a. PULSE NO. 1

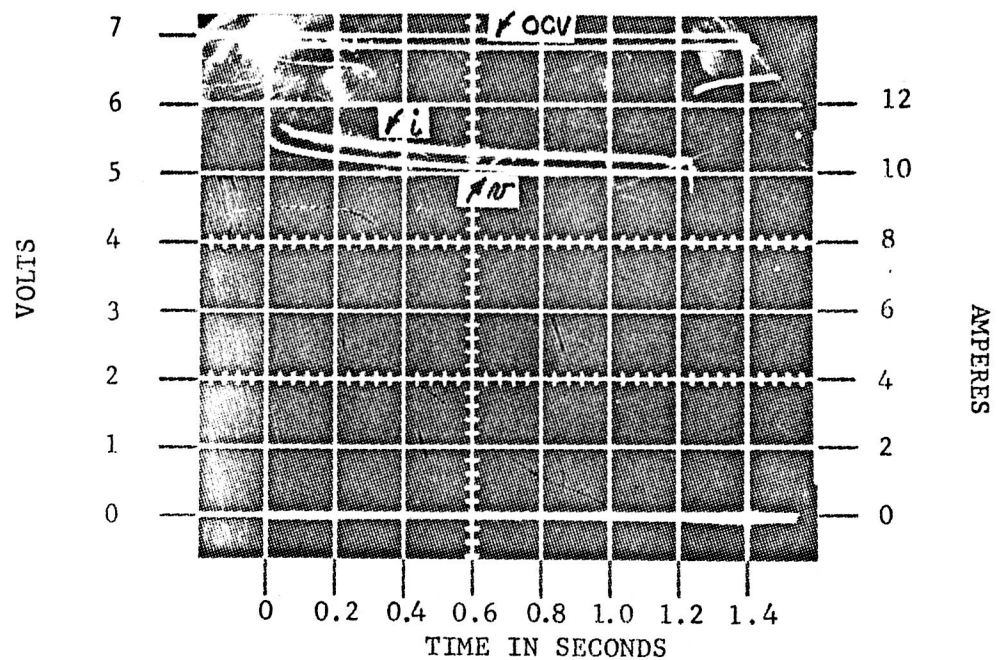


FIGURE 30b. PULSE NO. 2

OSCILLOSCOPE TRACES FOR TWO CONSECUTIVE PULSE DISCHARGES
OF A 5-CELL, SEALED, 2.76 IN² BIPOLAR BATTERY

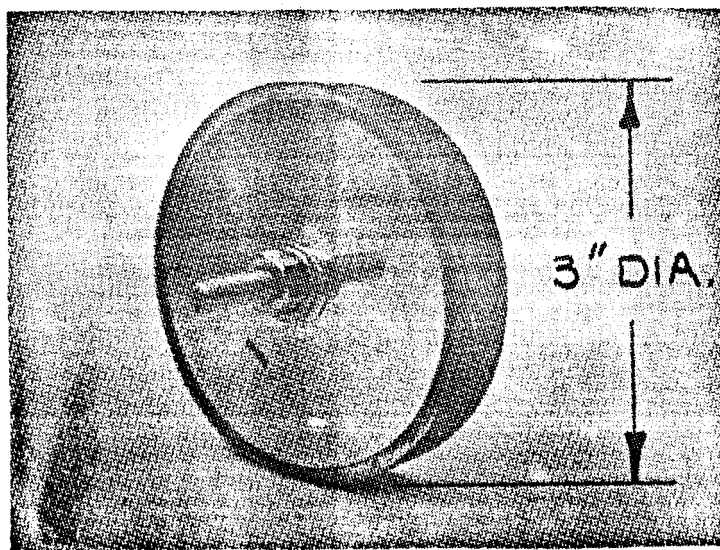


FIG. 31: 5-CELL, 10 AMP PULSE DISCHARGE
BIPOLAR BATTERY.

An encapsulated five cell battery was given ten pulse discharges before it was considered acceptable for delivery to NASA.

Figure 32 shows two consecutive pulses of a five-cell (encapsulated) battery with 2.76 in² of active area.

A total of ten developmental, five-cell modules were built. Seven had 3.1 in² of electrode area and three had 2.76 in² of electrode area. The average weight of a five-cell module (3.1 in², encapsulated) was 210 grams. Before encapsulation, the average weight of a sealed battery of the same size was 160 grams. The volume of five-cell sealed modules (3.1 in²) was 2.25 cubic inches, and 2.0 cubic inches for a 2.7 in² module, before encapsulation.

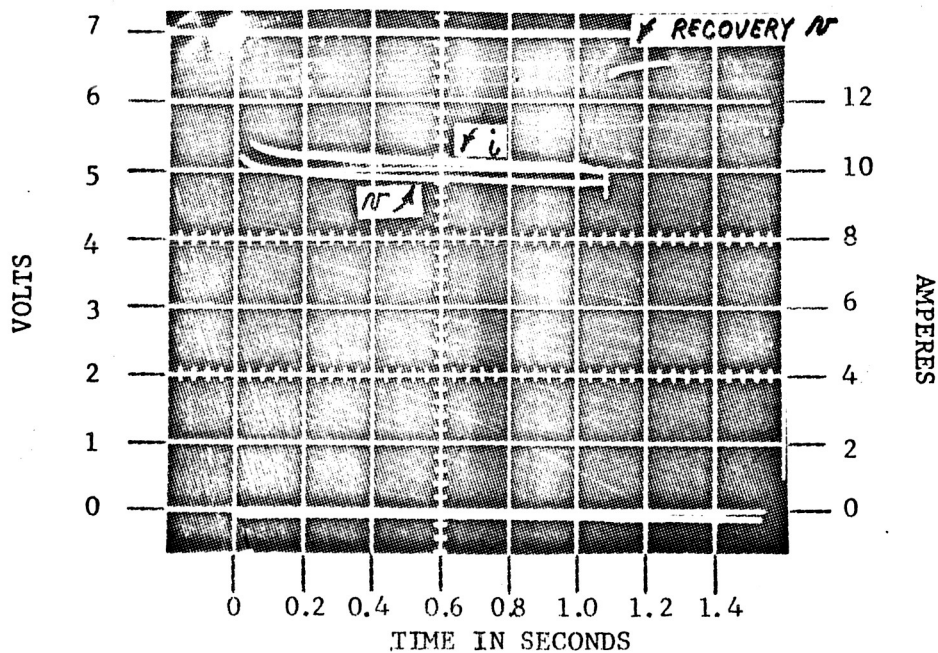


FIGURE 32a

PULSE NO. 1

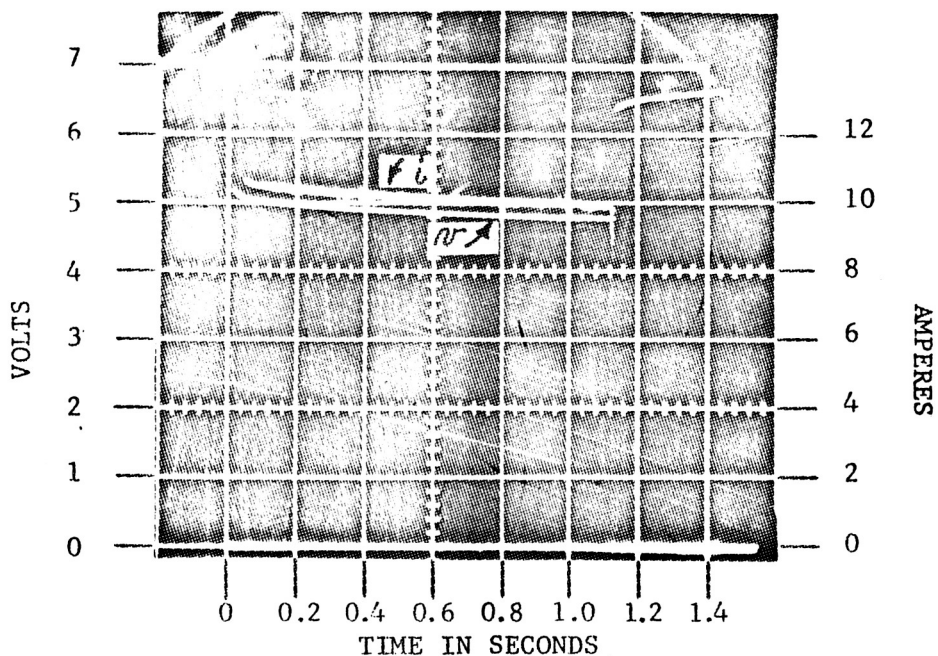


FIGURE 32b

PULSE NO. 2

OSCILLOSCOPE TRACES FOR 2 CONSECUTIVE PULSE DISCHARGES OF
A 5-CELL, 2.76 IN², SEALED AND ENCAPSULATED BIPOLAR BATTERY

DISCUSSION OF RESULTS AND CONCLUSIONS

The contractual objectives for the development of a 5 cell bipolar nickel-cadmium rechargeable battery with thick electrodes (30 mils sinter and 21 mils substrate) have been met and exceeded with a bipolar plate of 1-7/8" sinter diameter (2.76 in^2), at a current density of 3.62 A/in^2 , above 1.0 volts.

The five cell module has a nominal capacity of 300 mAh and is expected to yield 200 mAh (at the C/2 rate) when sealed, and several one second 10 ampere pulses, above one volt.

The reduced voltage, at subsequent pulse discharges, is primarily due to activation polarization at the negative, and concentration polarization at the positive electrodes, as evidenced by the oscilloscope traces. (Figure 13)

A thick sinter electrode (.030 inch) was developed which is capable of being impregnated with active materials to yield 150 mAh/in^2 of capacity at low rates. These electrodes can be manufactured in any size, from 2 in^2 to 100 in^2 , and in circular, square and rectangular shapes, not exceeding 8 inches in width of substrate. Larger sizes are limited by the present equipment in our laboratory. It is not necessary to use .021" thick substrate for the thick bipolar plates. Plates with .010 " substrate and .030" sinters can be produced in the sizes stated. However, it would be desirable to maintain the thicker substrate for the end plates, for added mechanical strength.

Of primary significance in this program was the development of a seal which bonds to the nickel substrate and stands up in the environment of the bipolar cell, although more cycle data are needed to ascertain its reliability and life.

The absence of a seal has prevented former investigators from building and testing rechargeable bipolar batteries. The development of the seal has, therefore, extended the state-of-the-art of bipolar battery technology.

Using the techniques developed, or extended on this program, more than ten rechargeable, sealed, five cell, bipolar nickel-cadmium batteries, were built with similar performance.

It would appear reasonable to conclude that bipolar batteries could be successfully produced, in quantity, in a variety of configurations, within practical size limitations, for high power pulse applications.

RECOMMENDATIONS

The bipolar battery system developed under this program was tailored to meet specific requirements. The system did not optimize the maximum power capability of the battery (which occurs at approximately 0.60 volts per cell).

Optimization of the nickel-cadmium bipolar battery system (where capacity is not a primary objective) will occur when development of thin plate electrodes are successfully incorporated into a sealed pulse discharge battery with an overcharge capability. Basic knowledge and experience in thin plate technology was acquired by Gulton from several in-house sponsored projects and from funded work (3).

The scope of this program did not permit the investigation of all the facets of this system. We recommend that investigation be continued in the following areas:

1. The effects of electrolyte concentration on activation and concentration polarization.
2. The effects of external pressure characteristics on high rate performance.
3. Efficient packaging design, which would include a pressure jacket to retain the stack, and prevent the electrodes from bending due to internal pressure build-up on charge. This in turn will prevent the creation of "hot spots" inside the cell.
4. The application of low density compressible non-woven separators with long life characteristics, into the bipolar sealed system.
5. The evaluation of bipolar cells with small reservoirs around the outer edges of the active material to hold the electrolyte during a low rate (C/10) overcharge.
6. It is possible to develop a system which would permit the battery to take a high rate overcharge without too great a sacrifice in volume. Charge control devices, as well as the incorporation of a Gulton developed third electrode (Adhydrode^(R)), to permit overcharge, were never investigated in relation to bipolar batteries. The application of such devices to bipolar batteries is highly desirable.

REFERENCES

1. Creighton, J., - Principles and Applications of Electrochemistry, (John Wiley and Sons, New York, 1944)
2nd Edition, Chapter 11, Paragraph 54.
2. Kapitza, P. L. - "A Method of Producing Strong Magnetic Fields", Royal Society of London Proceedings, A 105, 691-710, 1924.
3. Seiger, H. N.; Charlip, S.; Lyall, A. E.; and Cason, C., - "A Study of High Current Densities in Nickel-Cadmium Bipolar Batteries", Final Report, Contract DA-01-021 AMC-12509(Z), U. S. Army Missile Command, Oct., 1966.
4. Willinghamz, E. - "A Kapitza Type Nickel-Cadmium Battery", Fifth Quarterly Report, Contract No. AT(30-1)-1831, Atomic Energy Comission, 1956.
5. Tracey, V. A., and Williams, N. J. - "The Production Properties of Porous Nickel for Alkaline Battery and Fuel Cell Electrodes" Electrochemical Technology, January - February, 1965.
6. Ives, D. J. G., and Janz, G. J. - Reference Electrodes Theory and Practice, Academic Press, New York, 1961.

A P P E N D I X I

CALCULATIONS OF HEAT RISE DUE TO DISCHARGE CURRENT

APPENDIX

CALCULATIONS OF HEAT RISE DUE TO DISCHARGE CURRENT

Calculations have been performed to determine if discharges at 10 amperes for one second will cause excessive heat rise. It was felt that the 15 mA drain will cause no appreciable heat rise, and was, therefore, not considered as a problem requiring investigation.

The following assumptions were made on the analysis:

- a. All free energy is being converted to electrical power.
- b. The internal impedance is 1 milliohm.
- c. The specific heat of a bipolar battery is essentially the same as other nickel-cadmium batteries (.35 BTU/Lb./°F).
- d. The weight of a battery, used in the calculations, was 0.5 pounds.

From the equation:

$$\Delta H_f - \Delta F^0 = q$$

where: ΔH_f = (Heat of Formation) = 1.43 Cal/watt-hours

ΔF = (Free Energy of Formation) = 1.28 Cal/watt-hours

q = (Heat Dissipated or Absorbed) = -0.15 Cal/watt-hours

R = (Internal Impedance) = 1 milliohm

Discharge = 1 second at 10 amperes and 1 volt

= 10 watts x $\frac{1}{3600}$ hours = 2.7×10^{-3} watt-hours

Chemical Heat Generated = $(.15 \times 2.7 \times 10^{-3}) \times 3.4 \frac{\text{BTU}}{\text{watt-hour}}$
 = 13.7×10^{-4} BTU

Heat From I^2R = $100 \times .001 = 0.1$ watts

$0.1 \times \frac{1}{3600} = 2.7 \times 10^{-4}$ watt-hours
 = 8.18×10^{-4} BTU

Total Heat Generated = Chemical Heat + I^2R

= $10^{-4} (13.7 + 8.2) = 21.9 \times 10^{-4}$ BTU

Specific Heat = .35 BTU/Lb/°F

Weight of Battery = 0.5 lbs.

$$\text{Temperature Rise} = \Delta F = \frac{21.9 \times 10^{-4}}{3.5 \times 5 \times 10^{-2}} = 1.25 \times 10^{-2} \text{ } ^\circ\text{F}$$

It is apparent that this value is insignificant for the discharge.

DISTRIBUTION LIST

NASA/GODDARD SPACE FLIGHT CENTER REPORTS

National Aeronautics & Space Admin.
Scientific and Technical Information
Facility
College Park, Maryland 20740
Attn: NASA Representative
Send 2 copies plus 1 reproducible

National Aeronautics & Space Admin.
Washington, D.C. 20546
Attn: RNW/E. M. Cohn

National Aeronautics & Space Admin.
Washington, D.C. 20546
Attn: FC/A. M. Greg Andrus

National Aeronautics & Space Admin.
Goddard Space Flight Center
Greenbelt, Maryland 20771
Attn: Gerald Halpert, Code 735

National Aeronautics & Space Admin.
Goddard Space Flight Center
Greenbelt, Maryland 20771
Attn: Thomas Hennigan, Code 716.2
Send 3 copies

National Aeronautics & Space Admin.
Goddard Space Flight Center
Greenbelt, Maryland 20771
Attn: Joseph Sherfey, Code 735

National Aeronautics & Space Admin.
Langley Research Center
Instrument Research Division
Hampton, Virginia 23365
Attn: John L. Patterson, MS-234

National Aeronautics & Space Admin.
Langley Research Center
Instrument Research Division
Hampton, Virginia 23365
Attn: M. B. Seyffert, MS-112

National Aeronautics & Space Admin.
Lewis Research Center
21000 Brookpark Road
Cleveland, Ohio 44135
Attn: N.D. Sanders, MS 302-202

National Aeronautics & Space Admin.
Lewis Research Center
21000 Brookpark Road
Cleveland, Ohio 44135
Attn: M.J. Saari, MS 500-202

National Aeronautics & Space Admin.
Lewis Research Center
21000 Brookpark Road
Cleveland, Ohio 44135
Attn: R.R. Miller, MS 550-202

National Aeronautics & Space Admin.
Geo. C. Marshall Space Flight Center
Huntsville, Alabama 35812
Attn: Philip Youngblood

National Aeronautics & Space Admin.
Geo. C. Marshall Space Flight Center
Huntsville, Alabama 35812
Attn: Richard Boehme
Bldg. 4487-BB

National Aeronautics & Space Admin.
Manned Spacecraft Center
Houston, Texas 77058
Attn: William R. Dusenbury
Propulsion & Energy Systems Branch
Bldg. 16, Site 1

National Aeronautics & Space Admin.
Manned Spacecraft Center
Houston, Texas 77058
Attn: Richard Ferguson (EP-5)

National Aeronautics & Space Admin.
Manned Spacecraft Center
Houston, Texas 77058
Attn: Mr. Barry Trout

National Aeronautics & Space Admin.
Manned Spacecraft Center
Houston, Texas 77058
Attn: Forrest E. Eastman (EE-4)

National Aeronautics & Space Admin.
Washington, D.C. 20546
Attn: Office of Technology
Utilization

National Aeronautics & Space Admin.
Ames Research Center
Pioneer Project
Moffet Field, California 94035
Attn: Jon Rubenzer
Biosatellite Project

National Aeronautics & Space Admin.
Electronics Research Center
575 Technology Square
Cambridge, Mass. 02139
Attn: Dr. Sol Gilman

Jet Propulsion Laboratory
4800 Oak Drive
Pasadena, California 91103
Attn: Mr. Aiji Uchiyama

Department of the Army

U. S. Army Engineer R&D Labs.
Fort Belvoir, Virginia 22060
Electrical Power Branch
Energy Conversion Research Lab.

Commanding General
U.S. Army Weapons Command
Attn: AMSWE-RDR, Mr. G. Reinsmith
Rock Island Arsenal
Rock Island, Illinois 61201

U. S. Army Natick Laboratories
Clothing and Organic Materials Div.
Natick, Massachusetts 01760
Attn: G. A. Spano

Commanding Officer
U.S. Army Electronics R&D Labs.
Power Sources Division
Fort Monmouth, New Jersey 07003
Attn: Code SELRA/PS

Harry Diamond Laboratories
Room 300, Building 92
Conn. Ave. & Van Ness Street, N.W.
Washington, D.C. 20438
Attn: Nathan Kaplan

Department of the Navy

Office of Naval Research
Washington, D.C. 20360
Attn: Head, Power Branch, Code 429

Naval Research Laboratory
Washington, D.C. 20390
Attn: Dr. J. C. White, Code 6160

U. S. Navy
Special Projects Division
Marine Engineering Laboratory
Annapolis, Maryland 21402
Attn: J. H. Harrison

Naval Air Systems Command
Department of the Navy
Washington, D.C. 20360
Attn: Milton Knight (Code AIR-340C)

Commanding Officer
(Code QEWE, E. Bruess/H. Schultz)
U. S. Naval Ammunition Depot
Crane, Indiana 47522

Naval Ordnance Laboratory
Department of the Navy
Corona, California 91720
Attn: William C. Spindler (Code 441)

Naval Ordnance Laboratory
Silver Spring, Maryland 20910
Attn: Philip B. Cole (Code 232)

Commander, Naval Ship Sys. Command
Department of the Navy
Washington, D.C. 20360
Attn: C. F. Viglotti (Code 66605)

Commander, Naval Ship Sys. Command
Department of the Navy
Washington, D.C. 20360
Attn: Bernard B. Rosenbaum
(Code 03422)

Department of the Air Force

Flight Vehicle Power Branch
Aero Propulsion Laboratory
Wright-Patterson AFB, Ohio 45433
Attn: James E. Cooper

AF Cambridge Research Lab.
Attn: CRE
L. G. Hanscom Field
Bedford, Massachusetts 01731
Attn: Francis X. Doherty
Edward Raskind (Wing F)

Rome Air Development Center, ESD
Attn: Frank J. Mollura (RASSM)
Griffis AFB, New York 13442

Other Government Agencies

National Bureau of Standards
Washington, D.C. 20234
Attn: Dr. W.J. Hamer

National Bureau of Standards
Washington, D.C. 20234
Attn: Dr. A. Brenner

Office, Sea Warfare System
The Pentagon
Washington, D.C. 20310
Attn: G. B. Wareham

Mr. Donald A. Hoatson
Army Reactors, DRD
U. S. Atomic Energy Commission
Washington, D.C. 20545

Bureau of Mines
4800 Forbes Avenue
Pittsburgh, Pennsylvania 15213
Attn: Dr. Irving Wender

Private Organizations

Aerojet-General Corporation
Chemical Products Division
Azusa, California 91702
Attn: William H. Johnson

Aeronutronic Division of Philco Corp.
Technical Information Services
Ford Road
Newport Beach, California 92663

Aerospace Corporation
P. O. Box 95085
Los Angeles, California 90045
Attn: Library Acquisition Group

Allis-Chalmers Mfg. Co.
1100 South 70th Street
Milwaukee, Wisconsin 53201
Attn: Dr. P. Joyner

A. M. F.
Attn: Dr. Lloyd H. Shaffer
689 Hope Street
Springdale, Connecticut 06879

American University
Mass. & Nebraska Avenue, N.W.
Washington, D.C. 20016
Attn: Dr. R. T. Foley,
Chemistry Department

Arthur D. Little, Inc.
Acorn Park
Cambridge, Massachusetts 02140
Attn: Dr. Ellery W. Stone

Atomics International Division
North American Aviation, Inc.
8900 De Sota Avenue
Canoga Park, California 91304
Attn: Dr. H. L. Recht

Battelle Memorial Institute
505 King Avenue
Columbus, Ohio 43201
Attn: Dr. C. L. Faust

Bell Laboratories
Murray Hill, New Jersey 07971
Attn: U. B. Thomas

Bell Telephone Laboratories, Inc.
Whippany, N. J. 07981
Attn: D. O. Feder, Room 3B-294

The Boeing Company
P. O. Box 3868
Seattle, Washington 98124
Attn: Sid Gross, MS 85-86

Borden Chemical Company
Central Research Lab.
P. O. Box 9524
Philadelphia, Pennsylvania 19124

Burgess Battery Company
Foot of Exchange Street
Freeport, Illinois 61033
Attn: Dr. Howard H. Strauss

C & D Batteries
Division of Electric Autolite Co.
Conshohocken, Pennsylvania 19428
Attn: Dr. Eugene Willihnganz

Calvin College
Grand Rapid, Michigan 49506
Attn: Prof. T. P. Dirkse

Catalyst Research Corporation
6101 Falls Road
Baltimore, Maryland 21209
Attn: H. Goldsmith

ChemCell Inc.
150 Dey Road
Wayne, New Jersey 07470
Attn: Peter D. Richman

G. & W. H. Corson, Inc.
Plymouth Meeting
Pennsylvania 19462
Attn: Dr. L. J. Minnick

Cubic Corporation
9233 Balboa Avenue
San Diego, California 92123
Attn: Librarian
Mrs. Judy Kalak

Delco Remy Division
General Motors Corporation
2401 Columbus Avenue
Anderson, Indiana 46011
Attn: Dr. J. J. Lander

Douglas Aircraft Company, Inc.
Astropower Laboratory
2121 Campus Drive
Newport Beach, California 92663
Attn: Dr. George Moe

Dyntech Corporation
17 Tudor Street
Cambridge, Massachusetts 02139
Attn: R. L. Wentworth

E. I. DuPont De Nemours & Co.
Explosives Department
Repauno Development Laboratory
Gibbstown, New Jersey 08027
Attn: Mr. R. W. Prugh
(Contract NASw-1233)

Eagle-Picher Company
Post Office Box 47
Joplin, Missouri 64801
Attn: E. P. Broglio

Electric Storage Battery Co.
Missile Battery Division
2510 Louisburg Road
Raleigh, North Carolina 27604
Attn: A. Chreitzberg

Electric Storage Battery Co.
Carl F. Nroberg Research Center
19 West College Avenue
Yardley, Pennsylvania 19067
Attn: Dr. R. A. Schaefer

Electrochimica Corporation
1140 O'Brien Drive
Menlo Park, California 94025
Attn: Dr. Morris Eisenberg

Electro-Optical Systems, Inc.
300 North Halstead
Pasadena, California 91107
Attn: Martin Klein

Emhart Corporation
Box 1620
Hartford, Connecticut 06102
Attn: Dr. W. P. Cadogan

Engelhard Industries, Inc.
497 DeLancy Street
Newark, New Jersey 07105
Attn: Dr. J. G. Cohn

Dr. Arthur Fleischer
466 South Center Street
Orange, New Jersey 07050
Genral Electric Company
Schenectady, New York 12301
Attn: Dr. R. C. Ostoff/Dr. W. Carson
Advanced Technology Lab.

General Electric Company
Missile & Space Division
Spacecraft Department
P. O. Box 8555
Philadelphia, Pennsylvania 19101
Attn: E. W. Kipp, Room U-2307

General Electric Company
Battery Products Section
P. O. Box 114
Gainesville, Florida 32601
Attn: W. H. Roberts

General Electric Company
Research and Development Center
P.O. Box 8
Schenectady, New York 12301
Attn: Dr. H. Liebhafsky

General Motors-Defense Research Labs.
6767 Hollister Street
Santa Barbara, California 93105
Attn: Dr. J. S. Smatko/Dr. C. R. Russell

Globe-Union, Incorporated
P. O. Box 591
Milwaukee, Wisconsin 53201
Attn: Mr. J. D. Onderdonk
V. P. Marketing

Gould-National Batteries, Inc.
Engineering & Research Center
(Dr. D. Douglas)
2630 University Avenue, S.E.
Minneapolis, Minnesota 55418

Gulton Industries, Inc.
Alkaline Battery Division
212 Durham Avenue
Metuchen, New Jersey 08840
Attn: Dr. Robert Shair

Gulton Industries, Inc.
Alkaline Battery Division
212 Durham Avenue
Metuchen, New Jersey 08840
Attn: H. N. Seiger
Contract NAS W-12,300 only

Hughes Aircraft Corporation
Centinda Ave. & Teale Street
Culver City, California 90230
Attn: T. V. Carvey

Hughes Aircraft Corporation
Bldg. 366, M. S. 524
El Segundo, California 90245
Attn: P. C. Ricks

IIT Research Institute
10 West 35th Street
Chicago, Illinois 60616
Attn: Dr. H. T. Francis

Institute for Defense Analyses
R&E Support Division
400 Army-Navy Drive
Arlington, Virginia 22202
Attn: Mr. R. Hamilton

Institute for Defense Analyses
R&E Support Division
400 Army-Navy Drive
Arlington, Virginia 22202
Attn: Dr. G. Szego

Idaho State University
Department of Chemistry
Pocatello, Idaho 83201
Attn: Dr. G. Myron Arcand

Institute of Gas Technology
State and 34th Street
Chicago, Illinois 60616
Attn: B. S. Baker

International Nickel Co.
1000-16th Street, N.W.
Washington, D.C. 20036
Attn: Wm. C. Mearns

Johns Hopkins University
Applied Physics Laboratory
8621 Georgia Avenue
Silver Spring, Maryland 20910
Attn: Richard E. Evans

Johns Hopkins University
Applied Physics Laboratory
8621 Georgia Avenue
Silver Spring, Maryland 20910
Attn: Mr. Louis Wilson

Leesona Moos Laboratories
Lake Success Park, Community Drive
Great Neck, New York 11021
Attn: Dr. H. Oswin

Livingston Electronic Corporation
Route 309
Montgomeryville, Pa. 18936
Attn: William F. Meyers

Lockheed Missiles & Space Co.
Technical Information Center
3251 Hanover Street
Paló Alto, California 93404

Mallory Battery Company
Broadway & Sunnyside Lane
North Tarrytown, New York 10591
Attn: R. R. Clune

P. R. Mallory & Co., Inc.
Northwest Industrial Park
Burlington, Massachusetts 01803
Attn: Dr. Per Bro

P. R. Mallory & Co., Inc.
3029 E. Washington Street
Indianapolis, Indiana 46206
Attn: Technical Librarian

Martin Company
Denver Division
(Pl001, Mr. R. C. Wildman)
Mail No. P-6700-1
Denver, Colorado 80201

Martin Company
Electronics Research Department
P. O. Box #179
Denver, Colorado 80201
Attn: Williams B. Collins, MS 1620

Mauchly Systems, Inc.
Fort Washington Industrial Park
Fort Washington, Pennsylvania
Attn: John H. Waite

Melpar
Technical Information Center
7700 Arlington Blvd.
Falls Church, Virginia 22046

Metals and Control Division
Texas Instruments, Inc.
34 Forrest Street
Attleboro, Massachusetts 02703
Attn: Dr. E. M. Joe

Midwest Research Institute
425 Volker Boulevard
Kansas City, Missouri 64110
Attn: Physical Science Laboratory

Monsanto Research Corporation
Everett, Massachusetts 02149
Attn: Dr. J. O. Smith

North American Aviation Co.
S & ID Divison
Downey, California 90241
Attn: Dr. James Nash

Oklahoma State University
Stillwater, Oklahoma 74075
Attn: Prof. William L. Hughes
School of Electrical Eng.

Paul Howard Associates Inc.
Centerville, Maryland 21617

Power Information Center
University of Pennsylvania
4301 Market St., Rm. 2107
Philadelphia, Pennsylvania 19104

Power Sources Division
Whittaker Corporation
9601 Canoga Avenue
Chatsworth, California 91311
Attn: Dr. M. Shaw

Prime Battery Corporation
15600 Cornet Street
Santa Fe Springs, California 90670
Attn: David Roller

RAI Research Corp.
36-40 37th Street
Long Island City, N. Y. 11101

Radio Corporation of America
Astro Corporation
P. O. Box 800
Hightstown, New Jersey 08540
Attn: Seymour Winkler

Radio Corporation of America
AED
P.O. Box 800
Princeton, New Jersey 08540
Attn: I. Schulman

Radio Corporation of America
415 South Fifth Street
Harrison, New Jersey 07029
Attn: Dr. G. S. Lozier
Bldg. 18-2

Southwest Research Institute
8500 Culebra Road
San Antonio, Texas 78206
Attn: Library

Sonotone Corporation
Saw Mill River Road
Elmsford, New York 10523
Attn: A. Mundel

Texas Instruments, Inc.
P. O. Box 5936
Dallas, Texas 75222
Attn: Dr. Isaac Trachtenberg

TRW Systems, Inc.
One Space Park
Redondo Beach, California 90278
Attn: Dr. Herbert P. Silverman

TRW Systems, Inc.
One Space Park
Redondo Beach, California 90278
Attn: Dr. A. Krausz, Bldg. 60, Rm. 147

TRW, Inc.
23555 Euclid Avenue
Cleveland, Ohio 44117
Attn: Librarian

Tyco Laboratories, Inc.
Bear Hill
Hickory Drive
Waltham, Massachusetts 02154
Attn: Dr. A. C. Makrides

Unified Sciences Associates, Inc.
826 S. Arroyo Parkway
Pasadena, California 91105
Attn: Dr. S. Naiditch

Union Carbide Corporation
Development Laboratory Library
P.O. Box 5056
Cleveland, Ohio 44101

Electromite Corporation
Attn: R. H. Sparks
General Manager
562 Meyer Lane
Redondo Beach, California 90278

Union Carbide Corporation
Parma Laboratory
Parma, Ohio 44130
Attn: Dr. Robert Powers

University of Pennsylvania
Electrochemistry Laboratory
Philadelphia, Pennsylvania 19104
Attn: Prof. John O'M. Bockris

Westinghouse Electric Corporation
Research and Development Center
Churchill Borough
Pittsburgh, Pennsylvania 15235

Whittaker Corporation
3850 Olive Street
Denver, Colorado 80237
Attn: J. W. Reiter

Whittaker Corporation
Narmco R&D Division
3540 Aero Court
San Diego, California 92123
Attn: Dr. M. Shaw

Yardney Electric Corporation
40 Leonard Street
New York, New York 10013
Attn: Dr. Geo. Dalin

ADDENDUM TO OFFICIAL DISTRIBUTION LIST
FOR BATTERY REPORTS

<u>Addressee</u>	<u>No. of Copies</u>
NASA-Goddard Space Flight Center Greenbelt, Maryland 20771 Attention:	
Patent Counsel - Code 204	(1)
Office of the Director - Code 100	(1)
Office of the Assistant Director for Administration and Technical Services - Code 200	(3)
Office of the Assistant Director for Projects - Code 400	(1)
Office of the Assistant Director for Systems Reliability - Code 300	(1)
Office of the Assistant Director for Tracking and Data Systems - Code 500	(1)
Office of the Assistant Director for Space Systems - Code 600	(1)
Office of the Assistant Director for Technology - Code 700	(1)
GSFC Library - Code 252	(2)
Contracting Officer - Code 247	(1)
Technical Information Division - Code 250	(4)
Technical Representative - Code 716	Balance
NASA Headquarters FOB 10B Washington, D. C. 20546 Attn: Arvin Smith, Code RNW	